A NUMERICAL INVESTIGATION OF A TLP SYSTEM

A THESIS SUBMITTED TO
THE GRADUATE SCHOOL OF NATURAL AND APPLIED SCIENCES
OF
MIDDLE EAST TECHNICAL UNIVERSITY

BY

MELODİ NEŞE KOÇ

IN PARTIAL FULFILLMENT OF THE REQUIREMENTS
FOR
THE DEGREE OF MASTER OF SCIENCE
IN
CIVIL ENGINEERING

MAY 2022

Approval of the thesis:

A NUMERICAL INVESTIGATION OF A TLP SYSTEM

submitted by **MELODİ NEŞE KOÇ** in partial fulfillment of the requirements for the degree of **Master of Science** i**n Civil Engineering, Middle East Technical University** by,

Prof. Dr. Halil Kalıpçılar
Dean, Graduate School of **Natural and Applied Sciences** _____

Prof. Dr. Erdem Canbay
Head of the Department, **Civil Enginering, METU** _____

Assoc. Prof. Dr. Elif Oğuz
Supervisor, **Civil Engineering, METU** _____

Examining Committee Members:

Assoc. Prof. Dr. Nilay Sezer Uzol
Aerospace Engineering, METU _____

Assoc. Prof. Dr. Elif Oğuz
Civil Engineering, METU _____

Assist. Prof. Dr. Mehmet Adil Akgül
Civil Engineering, Yeditepe University _____

Assist. Prof. Dr. Ali Atashbar Orang
Mechanical Engineering, METU NCC _____

Assist. Prof. Dr. Redvan Ghasemlounia
Civil Engineering, Gedik University _____

Date: 06.05.2022

I hereby declare that all information in this document has been obtained and presented in accordance with academic rules and ethical conduct. I also declare that, as required by these rules and conduct, I have fully cited and referenced all material and results that are not original to this work.

Name Last name: Melodi Neşe Koç

Signature :

ABSTRACT

A NUMERICAL INVESTIGATION OF A TLP SYSTEM

Koç, Melodi Neşe
Master of Science, Civil Engineering
Supervisor : Assoc. Prof. Dr. Elif Oğuz

May 2022, 89 Pages

Renewable energy is becoming a popular research topic over the last decades. The floating wind turbine system consists of a typical wind turbine with a platform that the tower of the turbine is implemented. One of the popular floating systems is known as Tension Leg Platforms (TLPs). In this study, TLP is chosen due to the limiting nature of the system in terms of heave, roll and pitch motions. Due to the complexity of the system, coupling analysis of TLPs become important. In this thesis, a benchmark study in which a hydrodynamic analysis was carried out with SIMO, RIFLEX and WAMIT was taken as reference, and similar hydrodynamic analysis were carried out with ANSYS AQWA and HAMS. Fatigue, Aerodynamics, Structures and Turbulence (FAST) is one of the widely used open source code in order to carry out hydro, aero, servo, elastic coupling analysis of offshore wind turbine systems. FAST is used to analyze the TLP system, in this thesis. Three TLP designs are modeled and numerical calculations are performed under realistic environmental conditions in this thesis. Two of the six degree of motions, tendon tensions and natural periods are presented. The results of the three designs are compared with each other. Results of benchmark study and this thesis are compared and elucidate apparent similarity.

Keywords: Offshore Renewable Energy, Offshore Wind Energy, Tension Leg Platform Wind Turbine, Numerical Modeling

ÖZ

TLP SİSTEMİNİN SAYISAL İNCELENMESİ

Koç, Melodi Neşe
Yüksek Lisans, İnşaat Mühendisliği
Tez Yöneticisi: Doç. Dr. Elif Oğuz

Mayıs 2022, 89 Sayfa

Yenilenebilir enerji, son yıllarda popüler bir araştırma konusu haline gelmiştir. Yüzer rüzgar türbini sistemi, türbin kulesinin uygulandığı bir platforma sahip tipik bir rüzgar türbininden oluşur. Popüler yüzer sistemlerden biri Gergi Ayaklı Platformlar (TLP'ler) olarak bilinir. TLP, sistemin dalıp çıkma, yalpa, baş kıç vurma hareketleri açısından sınırlayıcı doğası nedeniyle seçilir. Sistemin karmaşıklığı nedeniyle, TLP'lerin kuplaj (birleştirme) analizi önemlidir. Bu tezde, SIMO, RIFLEX ve WAMIT ile hidrodinamik analizin yapıldığı bir araştırma referans olarak alınıp, benzer hidrodinamik analizler ANSYS AQWA ve HAMS ile yürütülmüştür. Fatigue, Aerodynamics, Structures and Turbulence (FAST), açık deniz rüzgar türbini sistemlerinin hidro, aero, servo, elastik bağlantı analizini gerçekleştirmek için yaygın olarak kullanılan açık kaynak kodlarından biridir. FAST ile sistem analizi tamamlanmıştır. Bu tezde, üç TLP tasarımı modellenmiş ve gerçek çevre koşulları altında sayısal hesaplamalar yapılmıştır. Tendon gerilimleri, altı serbestlik derecesindeki hareketlerden iki tanesi ve doğal periyotlar sunulmuş ve bu çalışmanın bulguları, referans çalışması ile karşılaştırılmıştır.

Anahtar Kelimeler: Açık Deniz Yenilenebilir Enerji, Açık Deniz Rüzgar Enerjisi, Gergi Ayaklı Rüzgar Türbini, Sayısal Modelleme

To my pretty mom …

ACKNOWLEDGEMENTS

I would like to express my deepest gratitude to my supervisor Assoc. Prof. Dr. Elif Oğuz for her guidance, advice, criticism, encouragements and insight throughout the research, and also thanks to Dr. Emre Uzunoğlu for his suggestions and comments.

I would also like to thank my esteemed lecturers who gave me a second chance in my thesis defense; Assoc. Prof. Dr. Nilay Sezer Uzol, Assist. Prof. Dr. Mehmet Adil Akgül, Assist. Prof. Dr. Ali Atashbar Orang, Assist. Prof. Dr. Redvan Ghasemlounia.

Mostly, I am grateful to my parents İlknur Başkılıç and Kayhan Koç for their love, confidence and encouragement they provided me not only throughout this thesis but throughout my life.

Finally, I would like to present my deepest thanks to my lovely friends Ayberk Şahin, Baharsu Akdağ, Barış Aktaş, Ceren Erol, Dilşen Kuzucuoğlu, Elif Karakoçak, Eyüp Sefercioğlu, İrem Bağcı, İrem Gökkaya, Merve Yeşilce, Sezin Kara and Ukte Yüksel.

Last but not least, thanks to Aytaç Osman Tosun for being with me.

TABLE OF CONTENTS

ABSTRACT vii

ÖZ ix

ACKNOWLEDGEMENTS xiii

TABLE OF CONTENTS xv

LIST OF TABLES xvii

LIST OF FIGURES xix

LIST OF SYMBOLS xxi

CHAPTERS

1 INTRODUCTION 1

1.1 Aim of the Study 12

1.2 Outline of the Thesis 13

2 LITERATURE REVIEW 15

3 RESEARCH METHODOLOGY 25

3.1 ANSYS AQWA 27

3.2 BEMRosetta and WAMIT 38

3.3 HAMS 40

3.4 FAST v8.16 41

4 NUMERICAL MODELING 45

4.1 Geometry and 3D model 45

4.2 Mass Properties 51

4.3 Mooring System 54
4.4 Environmental Conditions 56
5 RESULTS 59
5.1 General Comparison 60
5.2 Natural Periods and Surge RAO 62
5.3 Surge and Pitch Motions 66
5.4 Tendon Tensions 70
6 SUMMARY AND CONCLUSION 73
REFERENCES 75
APPENDICES
A. FAST Input Files for Free Decay Test of Surge Motion 81
B. FAST Input Files for Free Decay Test of Surge Motion 84
C. FAST Input Files for Free Decay Test of Pitch Motion 86
D. FAST Input Files for Free Decay Test of Pitch Motion 88

LIST OF TABLES

Table 1.1: Explanation of Abbreviations of methods in Figure 1.3. (Otter et al., 2021) 7
Table 1.2: Global Projects on Offshore Wind Energy (Erdozain, 2019) 8
Table 2.1: Environmental Conditions (Bachinsky, 2012) 20
Table 3.1: Floating Rigid Motion Descriptions (ANSYS, 2016) 35
Table 4.1: Geometrical Parameters of TLPWT Foundations (Bachinsky and Moan, 2012) 46
Table 4.2: Structural Steel Weight Approximations (Bachkinsky and Moan, 2012) 51
Table 4.3: Calculated Masses and Mass Moment of Inertias of TLPWT Components 52
Table 4.4: Mooring System Properties of Modeled TLPWT's (Matha, 2009) 54
Table 4.5: Environmental Conditions (Bachinsky and Moan, 2012) 56
Table 5.1: Mean Values of Surge, Pitch, Tendon Tension Ratio and Surge RAO Calculated in This Study with ANSYS AQWA 61
Table 5.2: Mean Values of Surge, Pitch, Tendon Tension Ratio Calculated in Bachinsky's Study (2012) 61
Table 5.3: Natural Periods and Surge RAOs of the Models 62

LIST OF FIGURES

Figure 1.1: Classification of Wind Turbine Platforms (Erdozain, 2019)..... 4
Figure 1.2: Offshore Platforms with Stabilization Methods (Butterfield et al., 2005) 6
Figure 1.3: A FOWT Structure (Otter et al., 2021)..... 7
Figure 2.1: 6 DOF Motions of TLPWT (Matha, 2009) 16
Figure 2.2: Conventional TLP design at left, Tension Based TLP design at the right (Bhaskara Rao et al., 2012)..... 18
Figure 2.3: TLPWT Designs (Bachinsky, 2012) 19
Figure 2.4: Geometry and Named Parts of the Model (Uzunoglu and Soares, 2020) 22
Figure 3.1: Flowchart of the thesis 26
Figure 3.2: Fluid Forces Represented in ANSYS AQWA (ANSYS, 2016)..... 33
Figure 3.3: Floating Rigid Motions (ANSYS, 2016)..... 34
Figure 3.4: Defined coordinate system and immersed body parameters used in HAMS (Yingyi, 2019) 41
Figure 3.5: FAST Simulation Overview and Modules (Jonkman et al., 2010) 43
Figure 4.1: Geometrical Parameters of TLPWT Foundations (Bachinsky and Moan, 2012) 46
Figure 4.2: AutoCAD Models of Proposed TLPWT Foundations 48
Figure 4.3: TLPWT1 Mesh Details Generated using ANSYS AQWA..... 49
Figure 4.4: TLPWT2 Mesh Details Generated using ANSYS AQWA..... 49
Figure 4.5: TLPWT3 Mesh Details Generated using ANSYS AQWA..... 50
Figure 4.6: TLPWT1 Mesh Views in RHINO..... 51
Figure 4.7: Mooring Line Location Parameters (NREL, 2009)..... 56
Figure 5.1: Free Decay Test Graph of TLPWT1 (FAST)..... 62
Figure 5.2: Free Decay Test Graph of TLPWT2 (FAST)..... 63
Figure 5.3: Free Decay Test Graph of TLPWT3 (FAST)..... 63
Figure 5.4: Free Decay Test Graph of TLPWT1 (FAST)..... 64
Figure 5.5: Free Decay Test Graph of TLPWT2 (FAST)..... 64

Figure 5.6:Free Decay Test Graph of TLPWT3 (FAST) 64
Figure 5.7: Natural Periods of TLPWTs in Surge 65
Figure 5.8: Surge RAO Graph of TLPWT1 (from ANSYS AQWA) 65
Figure 5.9: Surge RAO Graph of TLPWT2 (from ANSYS AQWA) 66
Figure 5.10: Surge RAO Graph of TLPWT3 (from ANSYS AQWA) 66
Figure 5.11: Pitch Motions of TLPWTs 67
Figure 5.12: Surge Motions of TLPWTs 68
Figure 5.13: Mean Surge Responses of TLPWTs 69
Figure 5.14: Mean Pitch Responses of TLPWTs 70
Figure 5.15: Mooring Lines Ratios of TLPWTs 70
Figure 5.16: Tendon Pairs of TLPWT1 - (a):T1-T2, (b):T3-T4, (c):T5-T6, (d):T7-T8 72

LIST OF SYMBOLS

SYMBOLS

A :	Cross section area (m^2)
A_{ij} :	Added mass coefficient (-)
$\overline{A_{ij}}$:	Normalized added mass coefficient (-)
a_w:	Amplitude of incident wave (m)
B_{ij}:	Damping coefficient (-)
$\overline{B_{ij}}$:	Normalized damping coefficient (-)
C_{ij}:	Hydrostatic force (kN)
$\overline{C_{ij}}$:	Normalized hydrostatic force (-)
D, D_1, D_2 :	Diameter of draft (m)
D_t :	Diameter of tendons (m)
g :	Gravitational acceleration (m/s^2)
h^2:	Square of the distance between two axes (m^2)
h_1 :	Length of draft (m)
h_p :	Spokes' or pontoons' height (m)
I:	Moment of inertia of the body (kg/m^2)
I_c:	Moment of inertia about the centre (kg/m^2)
L :	Length (m)
M :	Mass of the body (kg)

n_p : Number of pontoons or spokes (-)

ρ : Density of a fluid (kg/m^3)

R^2: Square of distance to central axis (m^2)

r_p : Radial distance from the tip of spoke or ponton to central axis of draft (m)

tt : Tickness of tendons (m)

T_t : Initial tendon tension (kN)

X_{ij} : Excitation force (kN)

$\overline{X_{ij}}$: Normalized excitation force (-)

V : Volume (m^3)

ω : Frequency (rad)

w_p : Spokes' or pontoons' width (m)

Z_s : Vertical location of pontoons or spokes (m)

γ: Specific weight (kN/m^3)

CHAPTER 1

INTRODUCTION

Renewable energy sources can be defined as natural sources that can produce energy with the faster rate than their energy consumption rate. Also, they are sustainable resources that can be found in nature profusely (van Vliet, 2012). Energy production from renewables is getting more attention and becoming an essential topic in recent years. In fact, the United Nations Department of Economic and Social Affairs (UN DESA) defines three critical parameters to ensure sustainable energy production. The keys of the goal are an accessible, reliable and affordable energy source and production. This point of view increases the efficiency of energy production and consumption, shareability of energy among the countries having the common interest. Various benefits of renewable energy have emerged from research and analysis of energy pathways for now and near future. Moreover, their conscious usage can decelerate the radical changes in the climate that fossil fuels have already contributed. (UN DESA, 2017). Yielding energy from renewables decreases the negative impacts of climate change. CO_2 emissions can be reduced by changing the consumed fuel type with less carbon-intensive sources. Economies shifting their energy consumption to low carbon-based supplies have a critical role in meeting the demand for climate stability in the world. The other advantages of renewable energy may be cost reduction in energy supply, pollution reduction and easiness of utilization instead of the complex energy production and supply (Afsharzade et al., 2016, Rezaei and Ghofranfarid, 2018). Thus, alternative resources have become more critical in reducing the dependence on fossil fuels, achieving CO_2 targets, and presenting both economic and environmental advantages (Riahi et al., 2012).

Moreover, traditionally used energy sources are limited and under extinction. Nature is constantly creating renewable energy sources.

There are some restrictions and drawbacks of renewable energy sources together with their advantages. The disadvantages are mainly because of renewable energy sources' natural characteristics. The project concept and energy production or transferring efficiency of a renewable source mostly depends on some factors such as its location, weather conditions, accessibility etc. These are critical limitations that show unpredictability and volatility of the sources. Quality assurance and production planning become challenges due to oscillations in energy capacity. And yet, the energy capacity of renewable energy projects are fallen behind the capacity of power plants consuming fossil fuels. There may be several reasons for the slow development, but the most significant one is the following. The produced daily total energy per renewable energy plant area ratio is generally lower than the same ratio of fossil fuel plants. In other words, there should be a larger plant area for a renewable energy project than a power plant with fossil fuels to produce the same amount of energy (Maradin, 2021).

The primary and commonly used renewable energy sources are geothermal, hydroelectric, biomass, wind, and solar energy (Gareiou et al., 2021). Renewable energy production was mainly focused on solar and wind energy in the 20th century. However, another source with high potential energy is slowly beginning to establish itself and arouse great interest from the scientific community. Wave energy and energy production from the ocean has become popular, and ocean energy research was included in the European Commission's development studies in the late 20th century (Lopez et al., 2013, Falcao et al., 2017). Knowledge of wind energy and arising interest in wave and ocean energy are combined, then a new concept emerged; offshore renewable energy. One of the most important offshore renewable energies is offshore wind because of the large amount of energy produced by state-of-the-art turbines. Generally, one wind turbine has one order of magnitude more

energy than one wave energy converter or the tidal energy device (Castro-Santos et al., 2017).

Wind energy can be converted into electricity using onshore and offshore turbine systems. In the last decade, offshore wind energy has become one of the most studied renewable energy sources due to its unique characteristics. Compared to onshore turbines, offshore wind farms have many advantages, such as achieving a more stable and higher wind speed to produce energy. Mainly, the wind power formula has the cube of wind velocity. Thus, a slight increase in wind speed creates a significant increase in the system's power efficiency (Oguz et al., 2013). In addition, land-based turbines also have some negative impacts, such as visual and noise pollution near the turbines and birds' migration routes. To avoid the harmful effects of land-based wind farms, many developed countries have attempted to establish offshore wind farms in the last decade (Oguz et al., 2013, Erdozain, 2019).

Offshore wind technology allows countries to take advantage of winds that have the high energy-producing capacity, generally due to their velocity and fetch distance. Also, wind farms are gigawatt-scale projects near the highly populated coastal areas common in many parts of the world. The gap between energy demand and supply may be decreased realizing massive energy production projects. Significant growth is expected in the offshore market in the following three decades. On a global scale, the total capacity of installed offshore wind facilities was 23 GW in 2018. Moreover, with the upcoming projects, global wind energy production capacity is expected to increase 228 GW in 2030 and almost 1000 GW in 2050 (IRENA, 2019).

On the other hand, offshore wind turbine concepts have numerous challenges in terms of economy and environment. The tourism sector may be a reason to reject wind turbine projects due to aesthetic concerns and noise pollution in coastal areas. Large distances from shore become an optimisation criterion to locate offshore wind turbines. However, the cost of projects is linearly increasing with the distance and

water depth. The initial investments in offshore wind turbines also grow, for that matter (Kausche et al., 2018).

Offshore wind turbine system mainly consists of two parts; a tower with a wind turbine on top and a platform where the tower is implemented. There are different platform types developed for different water depths, bathymetrical conditions etc. Location, environmental conditions, budget etc., are the topics that affect the selection of platform type. However, the most critical and restricting factor is water depth, because each platform is specialized for a specific depth. Mooring system design has a significant role in the development and specialization of floating systems. The most accounted problem while selecting the type of platform is stabilization due to the coupling effect of wind and wave. Because of that, platforms can be grouped regarding not to their shape but to their floatation principle. Mainly, there are four groups: single-point anchor reservoirs (SPARs), tension leg platforms (TLPs), semi-submersibles, and barges, as shown in Figure 1.1 as wind turbine platform type illustrations (Erdozain, 2019).

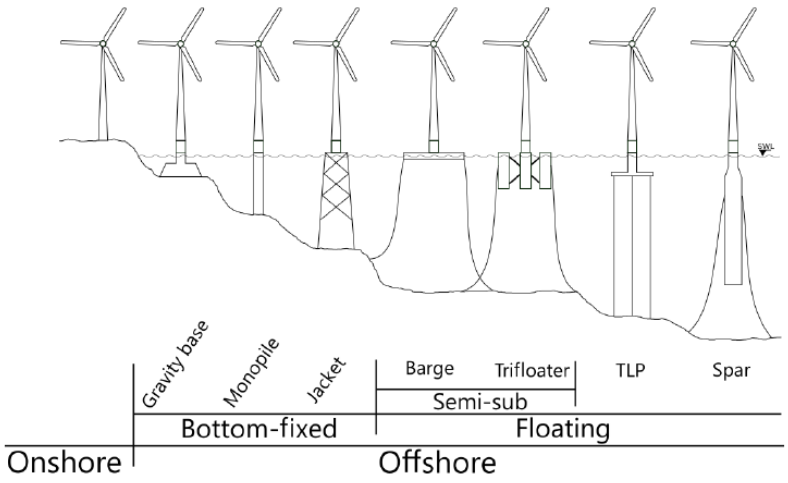


Figure 1.1: Classification of Wind Turbine Platforms (Erdozain, 2019)

Barge type has the largest waterplane area among mentioned platforms in Figure 1.1. Large waterplane area and low draft result in high hydrostatic restoring moments. The pitching motion results from large waterplane areas can lead to an adverse effect on turbines performance. Barge type does not have a big draft, so that they can be used in shallow depths easily. On the other hand, SPARs have the deepest draft. The floatation principle of SPARs is based on lowering the system's center of gravity below the buoyancy center. The goal of the concept can be ensured by adding sufficient weight to a significantly deep draft. In fact, the draft length can be reached to 120 m for 5 MW turbines. The coupling effect due to draft depth and turbine thrust force makes pitching motion critical. However, SPARs are appropriate to use in deeper water depths than other types shown in Figure 1.1. Semi-submersibles can be listed as a platform in between barges and SPARS in terms of geometrical properties such as waterplane areas and draft height. Semisubmersibles have large waterplane areas, but not as large as barges' and semisubmersibles have deep drafts, but not as deep as SPARs'. A series of columns are implemented beneath the waterplane area so that center of gravity is lowered and targeted moment of inertia is achieved. They do not need strong soil connections like TLPs and can resist pitching motion more than TLPs. However, installation of semisubmersibles is complex and material weight and expenses are high. TLP's do not require any deep draft that SPAR type has or waterplane area that barge type needs. Stabilization of TLPs is ensured with a mooring system and buoyancy forces. Figure 1.2. shows the main classifications of platform types considering stability (Uzunoglu and Guades Soares, 2020). Mainly, buoyancy forces and mooring lines are balanced with each other to fix the structure. Mooring lines are connected to the sea-bed in practice. However, there may be submersed structures between the floating platform and sea bed so that platform is connected directly to the submerged component before sea bed (Bhaskara Rao et al., 2012). Sea-bed should have a bearing that can resist tension in mooring lines. If the sea-bed soil is soft, gravity anchors can be used. Tension loss is named as slack condition which is not an acceptable issue. Slack problem may occur due to the high

dynamic load observed on mooring tendons. A sudden tension force created on tendons cause stability problem, after the cable experience tension loss (Uzunoglu and Guades Soares, 2020).

TLPWT platforms are generally considered for water depths between 70 m and 200 m. The appropriate lower limit for TLP (50m) is the upper limit for bottom fixed wind turbine systems. Also, TLP's upper limit of 200m is where the economic advantage of spar platforms begins (Bachinsky and Moan, 2012). Moreover, TLP system motions are limited so that transferred loads to the tower and blades are reduced in comparison with other floating systems (Butterfield et al., 2005, Robertson and Jonkman, 2011).

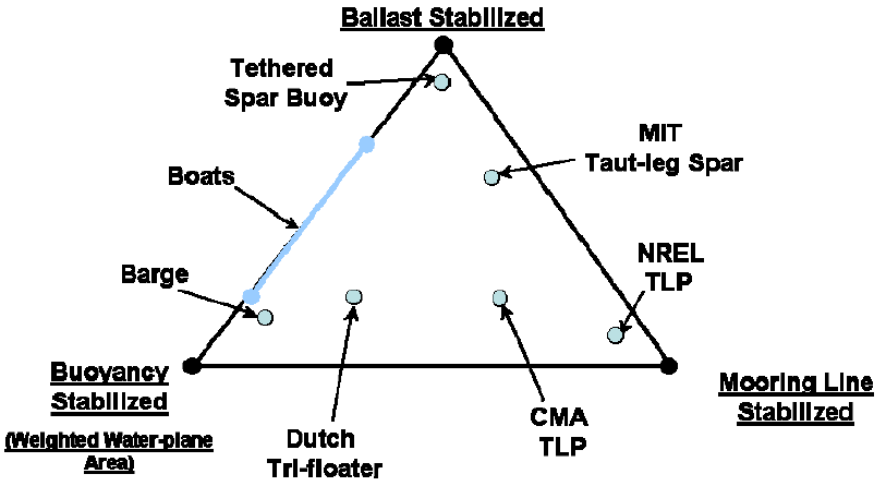


Figure 1.2: Offshore Platforms with Stabilization Methods (Butterfield et al., 2005)

Numerical modeling techniques and software vary for the preliminary design of floating wind turbines (FOWTs). With consideration to the phenomenon being studied and their tolerance limits, the choice of numerical modeling method will usually involve a trade-off between precision or integrity and processing efficiency. Precision and integrity conclude deviation of responses which are presented as a summary in general. FOWT system can be divided into three main components:

aerodynamics, structural dynamics, and hydrodynamics, in terms of numerical interpretation, as shown in Figure 1.3. Abbreviations of numerical computational methods mentioned in Figure 1.3. are tabulated in Table 1.1.

Integrity levels of numerical methods are subgrouped as low, mid and high. There is a linear relationship between fidelity and computational resource demand so that efficiency is reduced (Otter et al., 2021).

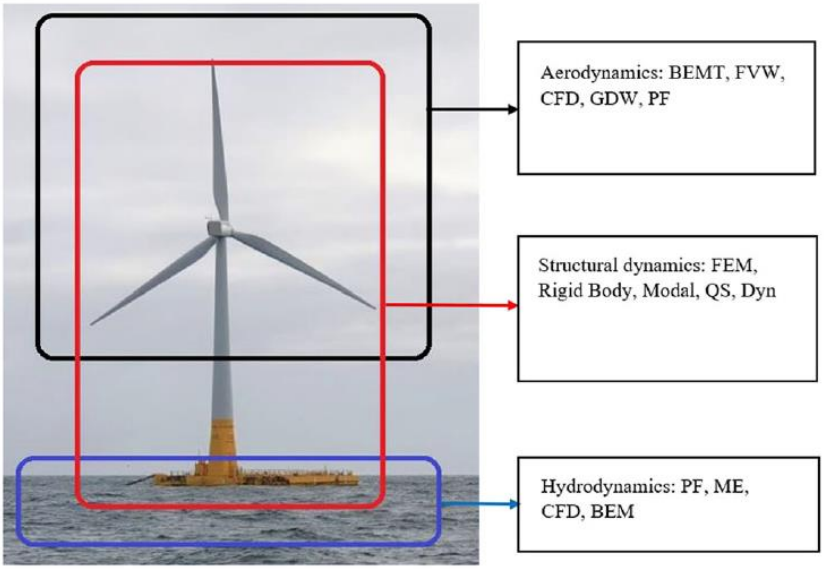


Figure 1.3: A FOWT Structure (Otter et al., 2021)

Table 1.1: Explanation of Abbreviations of methods in Figure 1.3. (Otter et al., 2021)

ACRONYM	*CATEGORY*	*FIDELITY*
BEM: Boundary Element Method	Hydrodynamic	Mid
BEMT: Blade Element Momentum Theory	Aerodynamic	Mid
CFD: Computational Fluid Dynamics	Aero-/hydrodynamic	High
Dyn: Dynamic method	Structural	Mid

FEM: Finite Element Method	Structural	High
FVW: Free Vortex Wake method	Aerodynamic	Mid
GDW: Generalized Dynamic Wake method	Aerodynamic	Mid
ME: Morison Equation	Hydrodynamic	Mid
PF: Potential Flow	Aero-/hydrodynamic	Mid
Q.S.: Quasi-Static method	Structural	Low

FAST, HAWC2, SIMA are commonly used engineering tools capable of solving coupled nonlinear aero-hydro-servo dynamics, aero-elastic and hydrodynamics, hydrodynamics and moorings subsequently. However, they require hydrodynamic coefficients' information from frequency domain (PF) solvers such as WAMIT, AQWA, Nemoh etc. for diffraction and radiation solution (Otter et al., 2021).

There is a lot of research focused on developing new and more stabilized models using numerical modeling methods. In fact, lots of projects and prototypes are constructed based on numerical and experimental studies. Some projects are decommissioned after test trials or operating for several years. Some projects are still working and producing energy.

Erdozain summarized the wind turbine projects constructed offshore in a doctoral thesis in 2019. Table 1.2. shows the offshore wind turbine projects that have a capacity of more than 15 kW (Erdozain, 2019).

Table 1.2: Global Projects on Offshore Wind Energy (Erdozain, 2019)

YEAR	*LOCATION*	*NAME*	*TURBINE*	*PLATFORM*	*ACTUAL STATUS*

2007	Apulia (Italy)	Blue H	80 kW	TLP	Decommissioned
2009	Karmøy (Norway)	Hywind 1	2.3 MW	Spar	Decommissioned
2011	Aguc¸adoura (Portugal)	WindFloat	2 MW	Semi-sub	Decommissioned
	Hordaland (Norway)	SWAY	15 kW	Spar	Decommissioned
	Maine (US)	VolturnUS	20 kW	Semi-sub	Decommissioned
2013	Nagasaki (Japan)	Kabashima	2 MW	Spar	Decommissioned
	Fukushima (Japan)	Mitsui	2 MW	Semi-sub	In Operation
2016	Fukushima (Japan)	Shimpuu	7 MW	Semi-sub	Decommissioned
2017	Fukushima (Japan)	Hamakaze	5 MW	Spar	In Operation
	Peterhead (Scotland)	Hywind 2	5 x 6 MW	Spar	In Operation
	Saint-Nazaire (France)	Floatgen	2 MW	Semi-sub	In Operation
2018	Fukuoka (Japan)	NEDO	3 MW	Semi-sub	Installation
	Aberdeenshire (Scotland)	Kincardine	2 MW	Semi-sub	In Operation

Blue H is the first scaled test prototype with TLP foundation and 80 kW power capacity. It was mounted at 113m water depth 21 km away from the coast. WindFloat had a semi-submersible platform with 2MW power. Hywind 1 is the first large-scale

project of FOWT with spar foundation installed at 220 m water depth. Hywind 2 is the first FWT farming project with spar foundation type. The constructed prototypes and projects are generally implemented on SPAR or semi-submersible platforms, rather than TLPs. It shows that TLP concept is not commonly used. The main challenge of the TLP concept is complexity during the adaptation of deep waters. Decommissioned projects in Table 1.2. did not pass trials generally due to malfunctioning or deficiency problems. (Erdozain, 2019). Spar system is more convenient to deep water and more expensive than other floating wind turbine foundation types at the same time (Uzunoglu et al. 2021).

In this thesis, TLP type is analyzed with some of the mentioned solution methodologies and computational techniques. For instance, comparison is carried out for three TLP foundations of 5 MW wind turbine, that National Renewable Energy Laboratory (NREL) proposed. These are the ones that Bachinsky analyzed in the benchmark paper. In this study, TLP systems defined in Baschinsky's paper are investigated and results are compared with the benchmark study. The scope is analyzing the TLPWTs using different available computer aided design program for hydrodynamics, which is ANSYS AQWA, instead of coded programs like SIMO and RIFLEX and comparing the outputs.

The hydrodynamic behavior of TLPs is investigated. Fatigue, Aerodynamics, Structures and Turbulence (FAST) open source code is a main processor for the analysis. However, hydrodynamic solution preprocessor part is changed from SIMO and RIFLEX to ANSYS AQWA. Moreover, WAMIT is commonly used hydrodynamic preprocessor of FAST. The recognized hydrodynamic input format (hydrodynamic coefficients) in FAST is the output format of WAMIT. Thus, FAST accepts files that have the format belike WAMIT outputs, only. In order to proceed, a basic computer application called BEMrosetta is used to convert AQWA output files to WAMIT output files directly for easy usage in FAST. The file extensions are changed with BEMrosetta to make FAST recognize input data from AQWA. The

crosscheck of transformation of AQWA results are done with a calculation spreadsheet which is prepared manually with the formulas mentioned in WAMIT guide.

In this thesis, three TLPWT designs are analyzed out of five mentioned in the benchmark study. Because, the last two designs defined in the benchmark study are commercial and their data are not publicly available. The first TLPWT platform design is NREL MIT design that is presented in Matha's master thesis (Matha, 2009). The second one is a modified version of Matha's proposal. Modification is performed by reducing leg numbers from four to three. The last one is half scaled version of SeaStar oil platform (Kibbee et al., 1999). The analysis is carried out using the same aerodynamic, hydrodynamic and environmental conditions. However, the geometrical and mass properties of each platform are different totally.

TLPWTs are compared with each other and with the results mentioned in Bachinksy's paper (Bachinsky and Moan, 2012). Response amplitude operators (RAO), tensions in mooring lines and radiation phenomena are identified and put in the graphs. The consistency and the relationship between the results are explained. Specifically, the surge motion and mooring line tension relationship is discussed for TLP system. Lastly, validation of interchanging between SIMO, RIFLEX, WAMIT and AQWA modules are discussed by comparing the outputs.

Additionaly, another hydroynamic preprocessor called HAMS is used to compare results obtained with AQWA. Similar hydrodynamic analysis is carried out with HAMS, also. Hydrodynamic behaviors of the three TLPWT models are obtained with HAMS, then coupling analysis is performed with FAST, same as the analysis carried out with AQWA. The results of the two hydrodynamic programs are compared with each other and differences are discussed.

1.1 Aim of the Study

TLPWT concept is relatively new among other renewable energy concepts. Numerous tools and methods have been investigated to accelerate the analysis and simulation process as well as understand the complexity of TLPWT's nature.

Generally, FAST is used to carry out coupled analysis of TLPWTs together with hydrodynamics programs such as WAMIT, Nemoh, SIMO and RIFLEX. They are all code-based simulation tools that the model is not visualized. AQWA has a user-friendly workbench with visualization tools. It is easier to get along with the FOWT concept with AQWA for a user in beginner level.

The purpose of this study is modeling and analyzing a benchmark case with a different hydrodynamic software. ANSYS AQWA software is used instead of SIMO, RIFLEX and WAMIT, which are specified in the benchmark study. The first reason for using ANSYS AQWA is its availability in the academy. Secondly, there is only a few research in the scope of coupling analysis that uses ANSYS AQWA as hydrodynamic preprocessor, in Turkey (Alkarem et al, 2018). Generally, ANSYS AQWA is used for only hydrodynamic analysis of vessels. Thus, this thesis aims to show the applicability and suitability of ANSYS AQWA in hydrodynamic analysis of floating wind turbines.

Moreover, an open source called HAMS is used as an alternative hydrodynamic analysis program to compare AQWA results. Following this, findings of (AQWA + FAST) are compared with the similar analysis carried out with (HAMS + FAST).

Bachinsky summarizes the milestone studies of TLP designs in a paper (Bachinsky and Moan, 2012). These designs are analyzed with the conventional methodology including SIMO, RIFLEX and AeroDyn which is a modul of FAST. Surge and pitch motions together with tendon tensions of mooring lines are investigated. Free decay tests are performed to ensure the elimination of resonance behavior by evaluating

RAOs. TLPWT motion results are compared with each other and also compared with corresponding solution results mentioned in the benchmark study. As a consequence, AQWA results of the thesis are generally matched with the results mentioned in the benchmark paper, as expected. Also, findings of HAMS open source code are observed as similar to results from AQWA. As a consequence, it is shown that AQWA or HAMS can be used instead of WAMIT in modeling TLPWT concept.

1.2 Outline of the Thesis

Hydrodynamic analysis and simulation of TLPWT concept are carried out with different modeling tools (ANSYS AQWA and HAMS) instead of a commonly used numerical programs (SIMO, RIFLEX, WAMIT) in this study. A brief information on renewable energy is given in introduction chapter together with description of floating platforms for offshore wind turbines. In Chapter 2, the Literature review concludes previous studies about TLPs including methodological and conceptual pieces of information, challenges and solution strategies. The methodology of this work is presented in Chapter 3 together with calculation principles of programs. In Chapter 4, modeling techniques, used software, 3D visualizations are presented. Geometrical and mass characteristics of designs together with environmental conditions are given. Results and discussions are given in Chapter 5. Lastly, Chapter 6 brings the study to a conclusion by summarizing the process and results.

CHAPTER 2

LITERATURE REVIEW

This chapter presents a comprehensive review of the literature, with a focus on the TLP system used in the offshore renewable energy sector. Also, the different methodologies, parameters that are considered for an optimum design of TLPs, modeling challenges etc., are defined. Several types of research have been carried out to get a better understanding of floating wind turbines. One of the common approaches is the linear frequency-domain approach. The term mainly refers to working with respect to frequency rather than time with only linear algebraic equations or solvers. 1.5 MW wind turbine is analyzed by Lee in 2005 with this technique. Jonkman explored different barge and TLP platform designs for various wind turbine models in 2011. Jonkman's study consists of varying TLP and spar buoy designs analyzed within the same environmental conditions. Dynamic coupling effect is investigated and optimum type of design is tried to identify. Although the designs are totally different, responses of TLP structures are similar. This shows stabilization technique (mooring system) has more effect on the dynamics of TLPWT system than design details. Moreover, the fatigue and ultimate loads observed on TLP and spar systems are similar. Only the tower is affected differently from the coupling loads. The exerted load on the tower of TLP system is observed less rather than other systems. The study shows the advantages of the newly born concept which is TLP and resolves the design trade-offs between floating system concepts. However, these studies are far from the reality due to not considering turbine properties. Research mentioned are focused on only the platform design and motion. Also, the linear approach does not give proper solutions to nonlinear behavior such as structural

dynamics, fully coupled aerodynamics and hydrodynamics response, second-order effects etc. (Matha, 2009).

Researchers at NREL proposed a new simulation tool that overcame problems that are mentioned before. This program consists of aerodynamic, hydrodynamic and servo elastic solutions and is named FAST (Jonkman, 2007). HydroDyn module of FAST works in the time domain to solve hydrodynamic effects such as nonlinear drag forces, sea currents, linear radiation and its components (added mass and damping), wave excitation forces.

To clarify the advantages and disadvantages of TLP system against the barge and spar buoys, a model of a 5 MW wind turbine with TLP stabilized platform is proposed by processing with FAST. ITI Energy barge, OC3 Hywind spar buoy and NREL TLP are compared in the same environmental conditions. The results indicate that barge is prone to high pitch and roll motions, so that turbine loads are observed much more than other concepts. The roll and pitch motion of the spar buoy platform is more remarkable than TLP's, but has an advantage in yaw motion. As a result, it can be said that TLP is more stable than others except for yaw motion. Motion axes and generally used coordinate systems can be seen in Figure 2.1. (Matha, 2009).

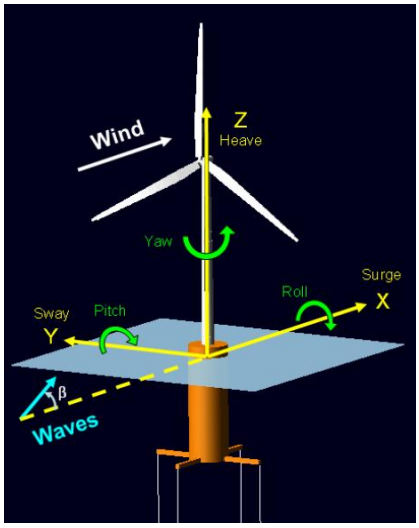


Figure 2.1: 6 DOF Motions of TLPWT (Matha, 2009)

In the last decades, the renewable energy sector has given tremendous interest and effort to offshore wind energy. The rising interest in the renewable energy sector

forces researchers to develop solutions and technologies. The high power generation capacity of winds blowing over deep-sea locations has encouraged lots of research about offshore wind energy. Foundation installation of a floating structure may be the most challenging part. Describing the behavior of the floating system that faces higher-order wave loads in deep-sea requires a design tool that can analyze the coupling effect of nonlinear excitations. A hybrid numerical model of TLP was proposed by Wehmeyer et al. in 2014 as an experimental study. Forces are described in linear potential theory, whereas hydrodynamic coefficients are accepted as nonlinear. According to Morison's equation, the Boundary integral equation method (BIEM) is used to solve hydrodynamic terms within the model. Forces due to radiation damping and added mass, which results from moving body in the water basically, are simplified with a freeware marine tool. The excitation force solution deals with the complex frequency domain describing loads exerted on the structure. ANSYS AQWA is used to determine the instabilities of excitation force. The hybrid numerical model is compared with the model prepared by only ANSYS AQWA for validation. A good match is observed. After the capability of the hybrid model is validated, a physical model is executed. Models match in terms of pitch motion. The general correlation between coefficients has an average of 88% (Wehmeyer et al., 2014).

Technological developments bring about unconventional designs and solution methodologies to the offshore wind turbine concept. Enhancement of an existing design may begin with overcoming its critical challenges and fulfilling gaps with different methods or structural additions. TLPs are sensitive to depth so that the motion responses in the vertical direction are generally essential. A hybrid foundation concept is proposed to be applicable in deeper waters than the usual TLPs' spectrum. Tension Based TLP (TBTLP) is a modified version of the regular TLP system (Bhaskara Rao et al., 2012). Traditional TLP concepts are upgraded and redesigned to generate minimal platforms to use TLPs in deep waters more than 200m depth (Kibbee ,1999). The minimal platform is combined with the tension base in the TBTLP concept. Required tendon length and weight to overcome extreme loads

increases with the water depth. Also, the stiffness of the system is reduced with longer tendons. The system becomes vulnerable to overtopping. The vessel size and waterplane should be increased to maintain sufficient buoyancy. TBTLP is proposed to work with an artificial sea-bed; sea-bed box as shown in Figure 2.2. Tension bed constraints the vertical and horizontal movement of tendons implemented on top. The double pendulum concept is used in TBTLP concept by maintaining the size of the hull near the water surface, so that tether slacking is avoided in deep water. A comparison and validation study is carried out for two different TLP designs using ANSYS AQWA. Tension bed implemented Norwegian TLP and SeaStar mini TLP are compared at 600m and 1200m depth (Bhaskara Rao et al., 2012).

Surge, heave and pitch motions results of the Norwegian and SeaStar designs are compared via ANSYS AQWA. RAOs of the conventional TLP which is at 600m and RAOs of TBTLP design at 1200m are observed as similar (Bhaskara Rao et al., 2012).

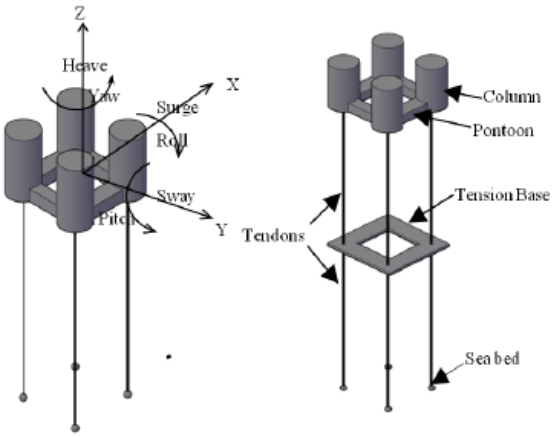


Figure 2.2: Conventional TLP design at left, Tension Based TLP design at the right (Bhaskara Rao et al., 2012)

Although there are extensive studies in the literature, the optimum design of a TLPWT has not been demonstrated. One of the studies in which different TLPWT models are analyzed under different environmental conditions to reach the optimum design is Bachinsky's study in 2012. State-of-the-art numerically modeled TLPWT designs are compared in terms of varying parameters. Five different baseline models

are numerically constructed within four different environmental conditions. Structural loads exerted on and observed in wind turbines and tendons are examined to discuss platform motions. Also, power production and cost-effectiveness are interpreted in a comparative manner among baseline designs (Bachinsky, 2012).

The first two designs are based on NREL MIT designs identified in Denis Matha's thesis (Matha, 2009). The mooring system of the first (NREL MIT - TLPWT1) is simplified as changing tendons from eight to four in total. Each tendon are assigned to each pontoon. The second one, named TLPWT2 is modified as a three-legged platform with %30 less initial tension in tendons than the first TLPWT model. The third baseline model TLPWT3 is a half-scaled version of SeaStar oil platform (Kibbee, 1999). The reference of the last two designs , TLPWT4 and TLPWT5, is the GLGH model (Henderson et al., 2010). All of the modeled designs can be seen in Figure 2.3.. Moreover, the only structural change is observed in tendon length due to the adaptation of the model to modeling water depth which is 150m (Bachinsky, 2012).

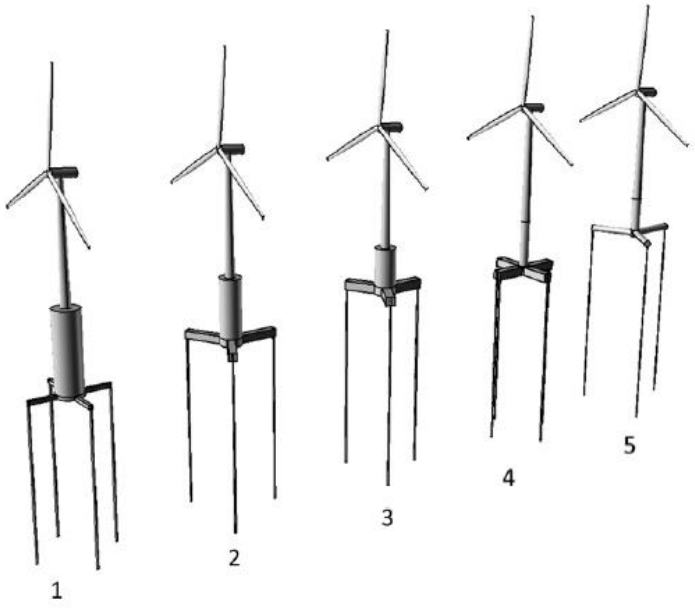


Figure 2.3: TLPWT Designs (Bachinsky, 2012)

Linear approach and approximations are performed while developing a spreadsheet to calculate the first predictions of TLPWTs. The spreadsheet calculations include

engineering assumptions and physical principles. Added mass matrix, mooring system stiffness matrix and hydrostatic stiffness matrix are calculated based on the example studies such as Chakrabarti and Hanna's added mass of a TLP work in 1990. Jain's study showed nonlinear coupled responses of a TLP in 1997 and Faltinsen's sea loads description in 1990. Tendons are accepted as straight and not affected by buoyancy changes. In calculations, heave hydrostatic stiffness depends on the waterplane area when the pitch and roll are based on the center of buoyancy and gravity and waterplane moment of inertia (Bachinsky, 2012).

After the linear approach and calculations, nonlinear coupled analysis is carried out with three different codes in Bachinsky's study in 2012. TLPWTs' are modeled in the time domain to determine their coupled behavior. AeroDyn module is performed with Generalized Dynamic Wake (GDW) and Blade Element Momentum (BEM) theories to establish moments and forces on blades (Moriarty and Hansen, 2005). Flexible elements such as tendons, shaft and tower are modeled with Riflex which is a finite element solver. Simo code models and analyses the hydrodynamics of the hull (MARINTEK, 2011).

Varying environmental conditions are specified in the study like TLPWT designs. Six environmental conditions are described and applied to each TLPWT (Bachinsky, 2012). Table 2.1. demonstrates the wind and wave conditions. Wave series are based on JONSWAP spectrum that significant wave height and period are the key elements (MARINTEK, 2011). TurbSim is used to generate 3D wind field (Jonkman,2009).

Table 2.1: Environmental Conditions (Bachinsky, 2012)

CONDITION	*1*	*2*	*3*	*4*	*5*	*6*
Mean wind speed at hub, *U* (m/s)	8.0	11.4	18.0	50.0	18.0	12.0
Turbulence intensity at hub, *I*	0.20	0.17	0.15	0.11	0.15	0.26
Significant wave height, *Hs* (m)	2.5	3.1	4.4	12.7	12.7	3.1
Peak wave period, *Tp* (s)	9.8	10.1	10.6	14.1	14.1	10.1

Wave and wind are acted on the TLPWTs in the same direction. Because of the aligned wave and wind forces, in-plane motions such as pitch, surge and heave become critical. The mean values of pitch and surge movements are calculated and compared with each other as well as the mean tendon tension. Moreover, free decay tests are performed for surge, yaw and heave motions.

Cost-effectiveness of a TLPWT can be determined from the displacement of the sytem and pretension of the tendons. The goal is generally to optimize the system with the lowest displacement and pretension possible. The mean pitch and surge values are mainly affected by mooring system stiffness. TLPWT5 has the most minor surge stiffness due to the small mean wave loads in comparison to the thrust force. On the other hand, TLPWT1 has the highest pitch stiffness due to its softest mooring system. Pitch motion affects the tension on tendons more than surge motion. As a consequence, tendons of TLPWT1 face the highest tension force.

Among all of the analyzed TLPWT designs in varying environmental conditions, TLPWT3 and TLPWT 4 are the most statically balanced and cost-effective designs (Bachinsky, 2012).

Power production from a floating system is challenging in terms of dynamics in that the platform provides sufficient motion stability. Significant pitching motion due to the waves and winds brings about deficiency in power production and power output fluctuations (Jeon et al., 2014). Pitch and heave movements are critical for most floating structures. However, the TLP system represents a rigid structure behavior because its mooring system depends on tension (Brennan et al., 2012). However, flotation stability is not sufficient for meeting the design requirements. The design process of a floating system platform should consider the ports and shipyards' water depth limits if it will be towed off shore. Lower transportation drafts become beneficial for this situation. The weights of the turbine and tower bring the center of the system's gravity higher. Platforms for heavy wind turbines should have the logical draft size and convenient dynamic responses while transporting the system to the installation site. A system that behaves like a barge while towing and performs as a

TLP after installation is proposed with design considerations, as can be seen in Figure 2.4. (Uzunoglu and Soares, 2020).

TLPs are specified with their mooring system based on tension force. The first critical point is that mooring lines are not sufficient alone to stabilize the whole system. The tension on mooring tendons mainly results from buoyancy forces. In conclusion, the mooring system and buoyancy forces exerted on the submerged portion of the platform combination stabilize the TLP system. Disadvantages of a TLP system are generally related to the transportation and installation process. Because, the mooring system can't work to stabilize the system before the installation. Additional barges idea arises as a solution to instability problem during towing (Uzunoglu and Soares, 2020).

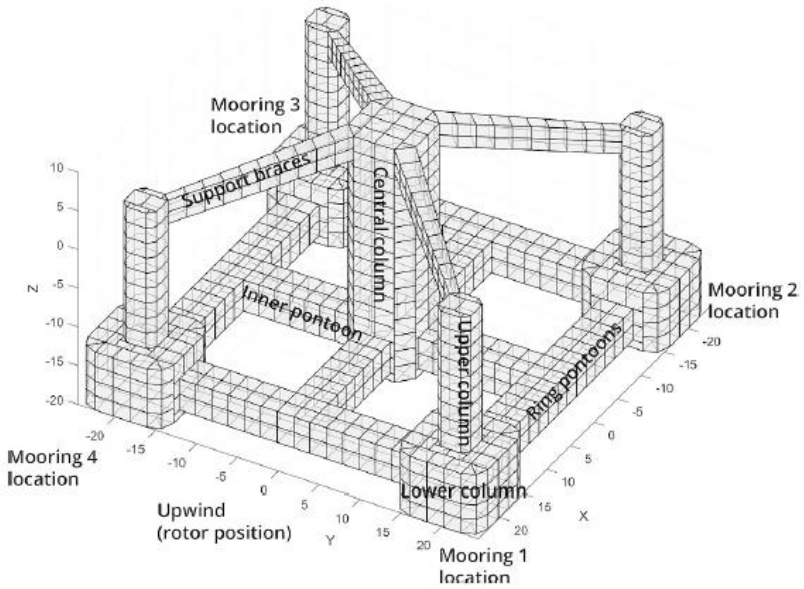


Figure 2.4: Geometry and Named Parts of the Model (Uzunoglu and Soares, 2020)

The proposed design platform is modeled under 10MW DTU turbine (Bak et al., 2013).

Design considerations for the free-floating condition can be summarized as follows;

- Draft of the platform should be small enough to be transported easily, even from shallow ports. Distance between the center of buoyancy of the platform and keel (KG) should be minor such as 5m.

- The platform model is tried to be lightweight.
- The reduction results from KG should be significant such as 90m approximately for 10MW DTU wind turbine.
- Decreased KG and additional ballast combination will increase floatation draft and displacement.

The design process is carried out with mainly three steps. ParMod creates a 3D model as a multi-purpose parametric with quadrilateral meshes. WAMIT (Lee and Newman, 2005) process is carried out for potential flow. FAST (Jonkman, 2007) computes platform behavior under the coupling effect in the frequency domain. Thrust forces caused by operating the turbine should be known for accurate frequency domain solutions. FAST model of 10MW wind turbine shared with the community by DTU and provides thrust values.

The model is analyzed under three different environmental conditions. Wind properties of the cases are rated wind speed, above rated wind speed and 50-year extreme values. JONSWAP spectrum is used to generate waves.

Results show that restrained responses within stability limits are established from the analysis of free-floating phase. The floating platform ensures the requirement mentioned previously. Slack behavior of mooring lines, breaking problems, or huge surge responses is not observed, so the intalled phase is considered safe. Moreover, the design overcomes the 50-year extreme conditions.

The essential advantage of a TLP system is its balanced state within the coupled motions, as mentioned in the previously explained studies. A carefully designed mooring system has a major role in that scope. TLPs tendons generally limit heave and pitch motions of the platform and surge and sway movements in the operating frequency range. The tendons' critical limiting states are mainly slacking and breaking. A broken tendon of a TLP situation is investigated in a study of Ren et al. in 2022. GustoMSC Tri floater platform is a reference of the failure simulation study. The NREL 5 MW wind turbine platform is adapted to 60m water depth, generally accepted as the shallowest recommended TLP installation depth (Ren et al., 2022). TLP designs are mainly constructed to depths more than 150m (Zhao et al., 2021).

The technical and economic limitations challenges are tried to overcome within shallow waters. Moreover, the multicolumn platform assures a high moment of inertia and sufficient buoyancy. Stabilization of the platform becomes achievable with proper TLP design. However, the coupling effect of the wind and waves can create complicated responses of the TLPWT system, resulting from a broken tendon. The dynamic responses are analyzed and tendon failure is investigated in terms of the safety of the damaged structure. The hydrodynamic properties of the system is computed, such as RAOs, natural frequencies, and tension forces in tendons (Ren et al., 2022).

FAST is used for complex body motions with processors WAMIT and ANSYS AQWA. Results show a good agreement between produced hydrodynamic coefficients such as added mass, excitation forces and damping coefficients of WAMIT and ANSYS AQWA. As a result, the reliability of the models is validated.

Free decay test is carried out to obtain the natural frequencies of the system (Ren et al., 2022). Natural periods are observed in the recommended range stated in specification DNVGL-RP-0286 as 15-60s for surge, 1,2s for heave, 2-5s for pitch and 8-20s for yaw (DNV, 2019).

The dynamic analysis shows a remarkable response in surge motion under survival conditions. Tension loss of broken tendon is reflected to other tendons. The dynamic and average factor of the tendon's safeties with the maximum tension is 1.11 and 2.04, subsequently. However, natural frequency of the system is still in the recommended range (Ren et al., 2022).

CHAPTER 3

RESEARCH METHODOLOGY

This chapter discusses the techniques used in both the benchmark and this study. The design concerns for TLPWT are outlined, along with the related theories. Hydrodynamic and coupled anlysis codes, simulations, and software are explained. Challenges of the TLPWT system and its numerical solutions are described.

TLPWT was primarily developed for its stability advantages. Mooring lines are used to stabilize TLPs rather than relying on buoyancy forces acting on the structure's draft. Due to the significant restriction of vertical and rotational motions, the wind turbine is well stabilized and exhibits minimum motion responses. TLP mooring line system can be used to regulate the most crucial modes (heave, roll, and pitch) of offshore structures. Under normal environmental conditions, all responses from these modes are in units of one (Jeon et al., 2014).

Additionally, the mooring lines contribute to the resonance behavior observed in restricted modes. The platform's resonance frequencies may decrease to high-frequency levels. Because surge, sway, and yaw motions are highly sensitive to variations in system frequency, the lengths of mooring lines should be carefully chosen to ensure safe frequency levels. Failures of the mooring system of TLPs can be primarily caused by two problems in particular; breaking and going slack. Breaking of a tendon may lead to instability problems. Slack is the term used to describe the tension loss in a mooring tendon, which can result in an abruptly large load when the tendon is brought back into tension (Uzunoglu and Soares, 2019).

As illustrated in Figure 3.1, a flowchart is created to depict the this study's work flow:

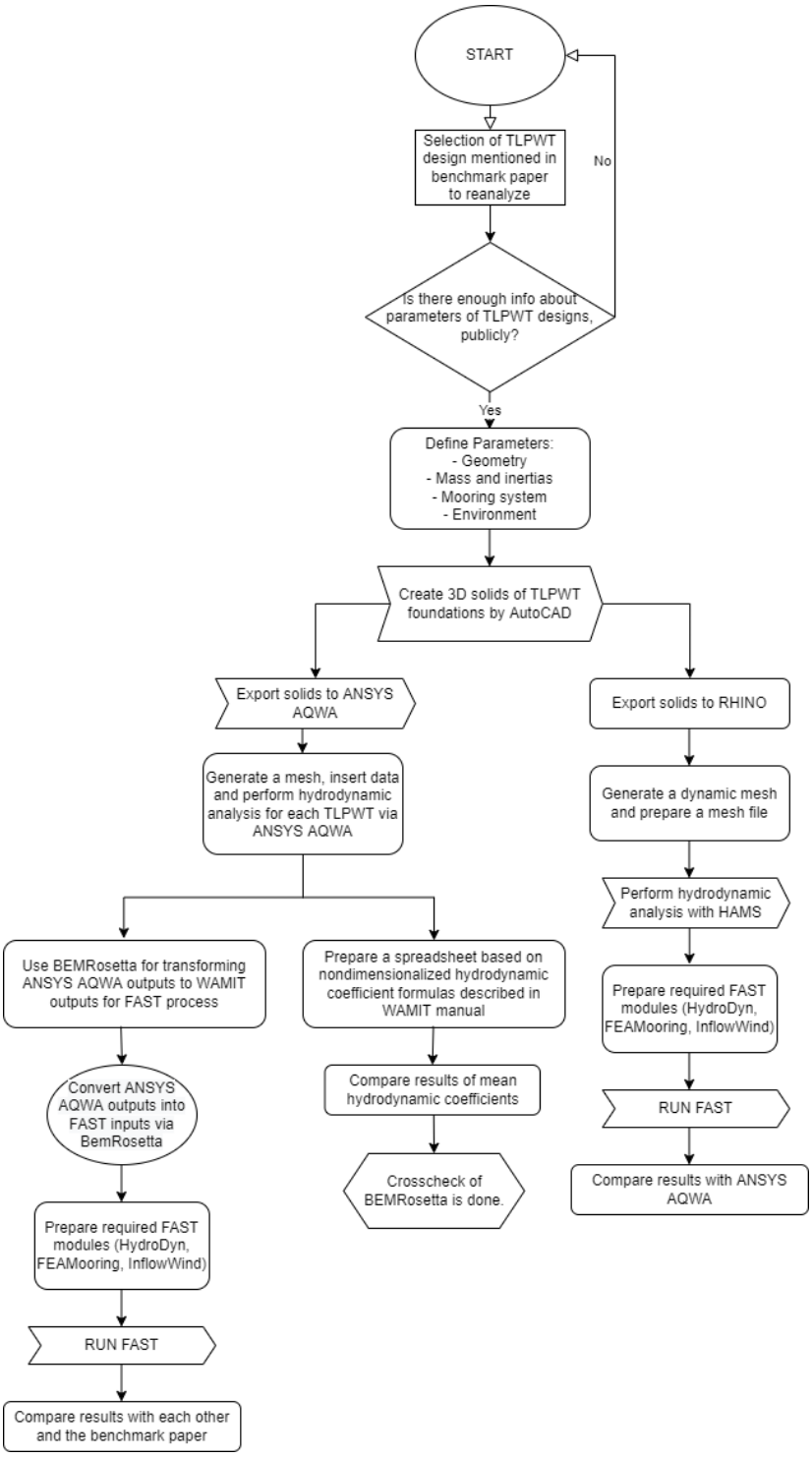


Figure 3.1: Flowchart of the thesis

The main aspect of this thesis is to determine whether ANSYS AQWA program as an appropriate hydrodynamic preprocessor in coupling analysis or not. For a better understanding and reliability of the results of ANSYS AQWA, another hydrodynamic analysis code called HAMS is used. Because, HAMS code is validated with a number of research in the literature. However, HAMS performs the analysis with the mesh file which is needed to be specified instead of geometry file of a model, unlike in the ANSYS AQWA process. At this point, RHINO program is used to prepare the mesh file of TLPWT models. RHINO can create mesh on the solid model which can be exported from AutoCAD.

Also, because ANSYS AQWA is not be able to produce outputs can be put directly in to FAST, and FAST only accepts certain input file type. Thus, an additional program had to be used. BEMRosetta converts the ANSYS AQWA output file type into the FAST input file type, directly. WAMIT program is generally used before FAST in order to obtain hydrodynamic coefficients. Thus, the manual of WAMIT presents several formulas to convert mentioned file types. Crosscheck of BEMRosetta is done with basic spreadsheet calculations based on the formulas in the WAMIT manual. However, analysis is not continued with FAST. Spreadsheet is used only for BEMRosetta crosscheck.

In the following subsections, theories and equations behind the main computer programs and codes used in this thesis are explained.

3.1 ANSYS AQWA

Numerous analysis and simulation methods can be used to determine the responses and forces exerted on the TLP structure and mooring system due to wave and wind. Boundary element method (BEM) is commonly used to obtain hydrodynamic coefficients because potential flow theory has limitations by its nature that are obvious and well-known such as linear approach and incapability of working with coupling forces or moments. Among other simulation methods such as smoothed

particle hydrodynamics (SPH) and computational fluid dynamics (CFD), it has become a better choice in the hydrodynamic perspective of TLPs due to the rapid processing of numerical simulations (Panelba, 2017). Boundary value problems are analyzed with boundary integral equations as a conventional method. Any numerical approach or method that can approximate and simplify the boundary integral equations is denoted as the boundary element method (BEM). BEM produces an approximate solution to the boundary value problem with an exact solution of differential equation in the domain. Additionally, the differential equation is parametrized using a finite set of parameters processing on the boundary (Costabel, 1987).

BEM can determine the hydrodynamic coefficients of a body or a platform under wave actions. The interaction of the body and the surrounding linear wave field generates radiated and scatter velocity potentials that can be addressed using BEM codes. The radiation potential comes with a moving body, whereas scattering potential exists when the body is fixed. Body motions can be obtained from the resolution of radiation potential that brings about radiation damping and added mass terms. BEM solvers can also produce excitation forces due to the wave action on the static body from scattering velocity potentials. BEM solvers are generally codes that can be supported with MATLAB scripts. The commonly used BEM solver codes for wave dynamics are WAMIT and NEMOH (Panelba, 2017). ANSYS AQWA is also a BEM solver software that solves wave energy problems and hydrodynamics. In practice, strip theory and 3D panel methods are generally used to calculate hydrodynamic loads. Hydrodynamic solutions of conventional ships and vessels are typically performed using strip theory. Accurate results can be obtained for classic ships and offshore structures. However, the strip theory may become insufficient for newly developed models. The method in ANSYS AQWA is based on potential theory, 3D panel method and surface is first discretized into diffraction panels, with singularities serving as boundary conditions. (ANSYS, 2016).

Ideal fluid conditions and linear hydrodynamic theory, which contribute to wave diffraction and radiation, are combined in fluid-structure interaction behavior described with following set of equations in the fixed reference axes;

- Laplace equation;

$$\Delta\varphi = \frac{\partial^2\varphi}{\partial X^2} + \frac{\partial^2\varphi}{\partial Y^2} + \frac{\partial^2\varphi}{\partial Z^2} = 0 \quad \text{(3.1.)}$$

applicable everywhere in the fluid domain, Ω.

- Linear free surface equation of zero forward speed case;

$$-\omega^2\varphi + g\frac{\partial\varphi}{\partial Z} = 0 \; on \; Z = 0 \quad \text{(3.2)}$$

- Body surface conditions;

$$\frac{\partial\varphi}{\partial Z} = \begin{cases} -i\omega n_j \;\; for\; radiation\; potential \\ -\dfrac{\partial\varphi}{\partial n} \;\; for\; diffraction\; potential \end{cases}$$

On the mean wetted body surface S_0. Here φ_1 represents the velocity potential function describing the initial incoming sinusoidal wave system.

- Seabed surface condition at depth of d;

$$\frac{\partial\varphi}{\partial Z} = 0 \; on \; Z = -d \quad \text{(3.3.)}$$

- A suitable radiation condition is added to the equations above so that, as $\sqrt{(x^2 + y^2} \to \infty$ indicates, the wave disturbance is diminished.

ANSYS AQWA computes the fluid velocity potential with respect to the equations above and controls the conditions by the use of boundary integration approach. Green's function is represented at a specific depth, as defined by the preceding equations and conditions. The velocity potential of diffraction and radiation waves can be written as a second-order Fredholm integral equation using Green's theorem. With the source distribution method applied to the wetted surface, the corresponding equation becomes as follows:

$$\frac{\partial\varphi(X)}{\partial n(X)} = -\frac{1}{2}\sigma(X) + \frac{1}{4\pi}\int_{S_0}\sigma(\xi)\frac{\partial G(x,\xi,\omega)}{\partial n(X)}dS \quad where\ X\epsilon S_0 \text{ .....(3.4)}$$

ANSYS AQWA performs with 3D panel method. In the scope of that, Hess Smith method is used in ANSYS AQWA to solve the equation above, in which the mean wetted surface is divided into quadrilateral or triangular panels. The resulting integral is denoted by:

$$-\frac{1}{2}\sigma_k + \frac{1}{4\pi}\sum_{Np}^{m=1}\sigma_m\frac{\partial G(X_k,\xi_m,\omega)}{\partial n(X_k)}\Delta S_m = \frac{\partial\varphi(X_k)}{\partial n(X_k)} \text{ .....(3.5)}$$

$$where\ X_k\epsilon S_0, k = 1, N_p, \omega_{min} = 0.001\sqrt{g/d}$$

Where N_p is the total panel number, ΔS_m is the area of mth panel, X_k, ξ_m are the coordinates of geometric center of the mth and kth panels respectively.

Panels are represented as meshes in ANSYS AQWA. Meshing is done with the Mesh module presented in ANSYS AQWA. The mesh is automatically generated on the bodies, and its density depends on maximum element size and tolerance. Two parameters are given manually to the ANSYS AQWA system. ANSYS AQWA automatically adjusts the compatibility of each mesh element to the body and wet surfaces. Tolerance input decides the negligibility of details. If the detail is smaller than tolerance value input, a single element may span over the detail. To avoid such kind of errors, element size should be decided carefully with regarding to the smallest details of bodies. ANSYS AQWA does not allow tolerance values greater than 60% of the maximum element size.

There is no choice between quadrilateral and triangular meshes in the basic mesh option. ANSYS AQWA determines the mesh type as needed. It is possible for the system to fail to generate meshes for complex structures. This time, the advanced option can be picked, and the entire process can be determined manually. Automatic meshing of the wetted surface or the entire body is possible with ANSYS AQWA's basic option. The 64-bit ANSYS AQWA version limits the mesh elements to 40000. The maximum element size, on the other hand, is tied to the maximum wave

frequency defined in ANSYS AQWA as a hydrodynamic input. The intended peak wave frequency is a meshing algorithm parameter. This value is the maximum frequency that the mesh system is allowed to have as the Maximum Allowed Frequency option. This value is one of the checkpoints used by ANSYS AQWA to validate its own operations. Additional checkpoints and quality assurance criteria in ANSYS AQWA for meshing are as the following:

- A sufficient number of quadrilateral and/or triangular panels should be used to represent the body/surface.

- Panel normals should be oriented perpendicular to the fluid field.

- The body/surface should be completely covered in panels with no overlaps or holes.

- Nonlinear time domain analysis takes the entire body into account. Both surfaces above and below the mean water level should be meshed as panels in such instances. The mean water level should not be low enough to cause damage to the panels.

Panels should meet the requirements for related equations;

- The panel area should be comparable to that of adjacent panels.

$$\frac{1}{3} \leq \frac{\Delta S_m}{\Delta S_k} \leq 3$$

$$m = 1, N_p + N_{lid}$$

Where ΔS_k denotes the area of any adjacent panel, N_p denotes the total number of panels, and N_{lid} is the total number of interior LID panels on the imaginary free surface (if it is specified).

- The aspect ratio of adjacent panels should not be too small.

$$C \frac{\Delta S_m}{L_{max}^2} \geq \frac{1}{3}$$

$$m = 1, N_p + N_{lid}$$

Where C equals one for quadrilateral panels and 2.3 for triangular panels, L_{max} denotes the longest side length of the m[th] panel, N_p denotes the total number of panels, and N_{lid} is the total number of interior LID panels of the imaginary free surface (if it is specified).

- Adjacent panel centers should avoid excessive closures.

$$d_{mk} \geq r_{fm}$$

$$m = 1, N_p + N_{lid}$$

Where d_{mk} is the distance between panel centers, r_{fm} is the radius of m[th] panel defined as $r_{fm} = \sqrt{\frac{\Delta S_m}{\pi}}$, N_p is the total number of panels , and N_{lid} denotes the total number of interior LID panels on the imaginary free surface (if it is specified).

- The panel should be small in size in comparison to the wave length.

$$L_{max} \leq \frac{1}{7}\lambda$$

Where L_{max} denotes the longest side length of m[th] panel.

Radiation and diffraction are the physical processes that result in fluid-induced loads, component of the hydrodynamic problem. The diffraction problem is concerned with the forces that excite waves. The diffraction notion is primarily concerned with two forces. The first one is the diffraction force created by the floating body distorting the coming wave. The second is Froude Krylov force which is observed on the floating body by the incident waves. Froude Krylov forces do not depend on the structure's geometry, but are based on the assumption that is non-distortionary of a coming wave when it is moving through the surface of the floating body. The explained process is visualized in Figure 3.2.

Incident waves oscillate the floating structure, which works as a counterweight to the fluid and transfers energy to it. This is known as the radiation issue. Calculations for transferred energy involve forces. To enable accurate identification of floating body motions, wave excitation forces should be combined with hydrodynamic damping and increased mass (Cekirdekci, 2015).

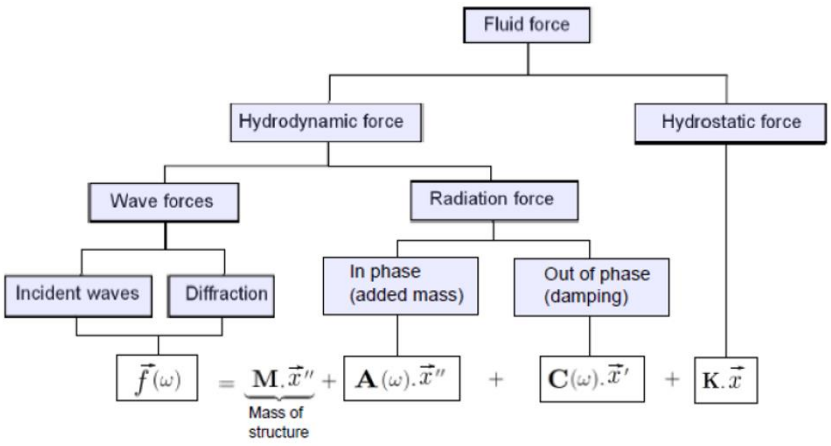


Figure 3.2: Fluid Forces Represented in ANSYS AQWA (ANSYS, 2016)

ANSYS AQWA calculates radiation and diffraction wave forces under the following linear potential theory assumptions:

- The forward velocity of the body/bodies is zero or negligibly small.

- The body/bodies are analyzed in an incompressible and inviscid fluid. Additionally, fluid flow is irrotational.

- All motions of the body/bodies are harmonic and in the first order. As a result, motions have a small amplitude.

Due to the first-order potential theory of radiation and diffraction, the velocity potential field may be formulized by the use of superposition theory as in Equation 3.6.

$$\Phi(\vec{X},t) = a_w \varphi(\vec{X}) e^{-i\omega t} \quad \text{.....(3.6.)}$$

where $\varphi(\vec{X})$ is an isolated space-dependent term, a_w is the incident wave's amplitude, and ω is the wave frequency.

Incident and diffracted waves are compounds of radiation waves resulting from body motion with six basic modes. They contribute to the isolated space-dependent term. Figure 3.3. and Table 3.1. illustrate the six modes in seakeeping theory. Six modes of body motions are affected by incident waves with unit amplitude as in Equation 3.2.

$x_j = u_j \ \ (j = 1,2,3)$

$x_j = \theta_{j-3} \ \ (j = 4,5,6)$ …….……(3.7.)

Equation 3.8 can be used to express the potential due to radiation, diffraction, and excitation waves.

$\varphi(\vec{X})e^{-i\omega t} = [(\varphi_1 + \varphi_d) + \sum_6^{j=1} \varphi_{rj} x_j]e^{-i\omega t}$……..……(3.8.)

where $\varphi(\vec{X})$ is an isolated space-dependent term, φ_1 denotes the first-order incident wave potential with unit wave amplitude, φ_d denotes the corresponding diffraction wave potential, and φ_{rj} is the radiation wave potential due to the j-th motion with unit motion amplitude.

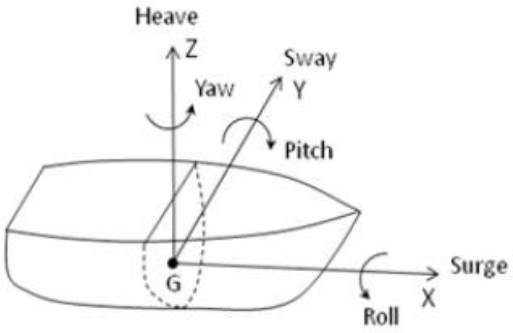


Figure 3.3: Floating Rigid Motions (ANSYS, 2016)

Table 3.1: Floating Rigid Motion Descriptions (ANSYS, 2016)

TRANSLATIONS	U_1	U_2	U_3
	Surge (Along X)	Sway (Along Y)	Heave (Along Z)
ROTATIONS	θ_1	θ_2	θ_3
	Roll (About X)	Pitch (About Y)	Yaw (About Z)

The first-order hydrodynamic pressure distribution (p^1) can be computed by Bernoulli's equation with the priorly calculated wave velocity potentials as in Equation 3.9. Various hydrodynamic forces can be evaluated by integrating the pressure distribution along with the wetted surface.

$$p^1 = -\rho \frac{\partial \phi(\vec{X},t)}{\partial t} = i\rho\omega\varphi(\vec{X})e^{-i\omega t} \quad \text{(3.9.)}$$

where $\varphi(\vec{X})$ is isolated space-dependent term, $\Phi(\vec{X},t)$ is denotes the velocity potential field, and ρ denotes the water density.

The total first-order hydrodynamic force can be composed as in Equation 3.10. Where j is =1,6, ω is the wave frequency, and S is the wetted surface.

$$F_j = [(F_{Ij} + F_{dj}) + \sum_{k=1}^{6} F_{rjk}x_k] \quad \text{(3.10.)}$$

F_{Ij} is Froude-Krylov Force of j[th] mode as in Equation 3.11.

$$F_{Ij} = -i\omega\rho \int_{S_o} \varphi_I(\vec{X})n_j dS \quad \text{(3.11.)}$$

F_{dj} is diffraction force of j[th] mode as in Equation 3.12.

$$F_{dj} = -i\omega\rho \int_{S_o} \varphi_d(\vec{X})n_j dS \quad \text{(3.12.)}$$

F_{rjk} is radiation force of j[th] mode due to radiation caused by motion in k[th] mode as in Equation 3.13.

$$F_{rjk} = -i\omega\rho \int_{S_o} \varphi_{rjk}(\vec{X}) n_j dS \ldots\ldots\ldots\

AutoCAD models a solid body as a full body with an exact volume. AQWA, on the other hand, deals with tin bodies with no thickness, the masses and inertias of which are defined independently. Thus, several modification tools in AQWA's Geometry module convert exported bodies to AQWA-usable bodies.

AQWA's hydrodynamic diffraction module generates solutions and responses with precise mass and inertia values inside a specific hydrodynamic condition. In AQWA, solid bodies are characterized using geometrical data, whereas mass and inertia are defined manually. Previous studies can be used to determine the density of materials for this thesis (Bachinsky and Moan, 2012). Characteristics such as mass and inertia data can be calculated using spreadsheet calculations considering solid geometries. Mass can be calculated by multiplying the density by the volume. Additionally, the cylinder's basic inertia formula and parallel axis theorem can be applied to obtain final inertias.

AQWA specifies the environmental effects as mostly wave and wind. To acquire correct results, wave, wind, and sea state variables are specified. While analyzing, Significant wave height, peak period, and water depth are critical wave properties to consider. These parameters are precisely stated in AQWA, and then the required and desired frequency margin is calculated. In AQWA, multi-directional waves, commonly known as short crested waves, are denoted by Equation 3.17.

$$\zeta(X,Y,t) = \sum_{m=1}^{N_d} \sum_{j=1}^{N_m} a_{jm}\, e^{j(k_{jm}XcosX_m + k_{jm}YsinX_m - \omega_{jm}t + \alpha_{jm})} \quad \text{.....(3.17.)}$$

where ω_{jm} is the wave frequency, a_{jm} denotes the wave amplitude, and α_{jm} denotes the phase angle. N_d denotes the wave direction number, N_m denotes the wave components along each of the wave directions X_m $(m = 1, N_d)$, and k_{jm} denotes the wave number.

A completely characterized sea state requires a few statistical characteristics similar to those found in wave spectra. The spectrum of the JONSWAP (Joint North Sea Wave Project) can be used to model an imbalanced situation caused by energy flow

in the wave system. In general, the combination of high wind speed and waves generates unbalanced energy. In AQWA, the JONSWAP spectrum can be described by its beginning and ending frequencies. Equation 3.18 defines the starting frequency, while Equation 3.19 defines the ending frequency.

$$\omega_s = \omega_p(0.58 + 0.05\frac{\gamma-1}{19}) \quad (3.18.)$$

$$\omega_f = \omega_p F(\gamma) \quad (3.19.)$$

Where γ is the weighting function whose values are tabulated in ANSYS, 2016.

Wind fields, as well as waves, can be defined in AQWA. Required uniform wind parameters are mean wind velocity (speed or amplitude) and direction (at 10m above the water surface). Wind fields are assumed to be uniform within a given height and unidirectional.

Connections and mooring systems can be defined in AQWA workbench. Tether or catenary mooring line properties can be assigned to the mooring system with appropriate mooring line connections so that diffraction analysis can be carried out more realistically (ANSYS, 2016). However, in this study, the mooring system is not modeled using AQWA to ensure that the hydrodynamic coefficient solution does not diverge from the objective. Also, the tether properties used as inputs by FAST are often elementary data such as tether stiffness, tendon stiffness, and unstretched length. However, AQWA requires a completely defined mooring system, complete with connection stiffness, accurate coordinates for tendon connections, and so on. As a result, the mooring system is analyzed using FAST's mooring analysis module, FEAMooring.

3.2 BEMRosetta and WAMIT

As mentioned in the general research methodology section, since ANSYS AQWA is not be able to produce outputs can be put directly in to FAST, and FAST only accepted certain input file type, BEMRosetta is used. Mentioned process in ANSYS

AQWA subsection are needed to obtain hydrodynamic coefficients which may be tabulated as outputs after carrying out hydrodynamic analysis. However, added mass, excitation forces, and radiation damping outputs are not given by ANSYS AQWA as the same format as WAMIT outputs used in the FAST process. As a solution, the AQWA outputs are converted to WAMIT output format by using an open-source code named BEMrosetta. This code only rearranges the hydrodynamic data and presents them in the tabulated form.

WAMIT is generally used before FAST as a hydrodynamic preprocessor. Thus, the manual of WAMIT presents several formulas to convert mentioned file types as FAST inputs. Crosscheck of BEMRosetta is performed with basic spreadsheet calculations based on the formulas in the WAMIT manual. Spreadsheet is only used for crosscheck between BEMRosetta outputs and outputs that can be obtained with WAMIT formulas.

WAMIT manual implies formulas for the correct output type of hydrodynamic coefficients. A basic spreadsheet is used to normalize and transform nondimensional data from the AQWA output format to the WAMIT output format. Equation (3.20.) and (3.21.) represent normalization and nondimensionalization of the added mass and the damping coefficients. Equation (3.22) can be used to normalize excitatory forces, RAOs, whereas Equation (3.23) can be used to normalize hydrostatic forces (WAMIT, 2013). WAMIT formulas and BEMrosetta gives the same outputs to be used for FAST. This method is used to validate results of WAMIT handbook and BEMrosetta.

$$\overline{A_{ij}} = \frac{A_{ij}}{\rho} \quad \text{(3.20.)}$$

$$\overline{B_{ij}} = \frac{B_{ij}}{\rho\omega} \quad \text{(3.21.)}$$

$$\overline{X_{ij}} = \frac{X_{ij}}{\rho g A} \quad \text{(3.22.)}$$

$$\overline{C_{ij}} = \frac{C_{ij}}{\rho g} \quad \text{(3.23.)}$$

Nondimensionalization of added mass (A_{ij}), damping (B_{ij}), excitation forces ($\overline{X_{ıJ}}$) and hydrostatic restoring coefficients (C_{ij}) are calculated using the density of water (ρ), frequency in radians (ω), gravitational acceleration (g), and cross-sectional area (A). Nondimensionalized forms of added mass, damping, excitation forces, and hydrostatic restoring coefficients are denoted as A_{ij}, $\overline{B_{ıJ}}$, $\overline{X_{ıJ}}$ and $\overline{C_{ıJ}}$.

3.3 HAMS

Hydrodynamic Analysis of Marine Structures (HAMS) is an open-source code for the numerical computation of the wave effects. It is based on boundary integral equations in the potential flow theory for analysis of wave-structure interactions. It is written in FORTRAN 90 (Yingyi, 2019).

Because, HAMS is a verified and validated hydrodynamic analysis code in the literature, it is only used to compare ANSYS AQWA results in the scope of this thesis. General assumptions and theories behind HAMS are presented as following;

- The flow is assumed to be inviscid, free of separation or lifting effects, irrotational, and incompressible. In this potential flow framework, the flow is described by a velocity potential;

  $$\varphi(x, y, z) = \varphi_i + \varphi_d + \varphi_r$$

  Where φ_i is incident wave potential, φ_d is diffracted wave potential, φ_r is radiated wave potential.
- The above velocity potentials satisfy the Laplace equation in the entire fluid domain mathematically, as specified in ANSYS AQWA section with Equation 3.1.
- Subjected boundary conditions are respectively at the free surface, on the body surface, at the sea bottom, and in the far field, as shown in Figure 3.4., which can be expressed as;

  $$\nu * \varphi = \frac{\partial \varphi}{\partial z} \quad , \qquad z = 0$$

$$V_n = \frac{\partial \varphi}{\partial n}$$

$$0 = \frac{\partial \varphi}{\partial z} \quad , \qquad z = -h$$

Where $\nu = \omega^2/g$ is the wave number in the deep water, g is the gravitational acceleration, V_n is the normal velocity at a specific point on submersed body, h is the water depth (Yingyi, 2019).

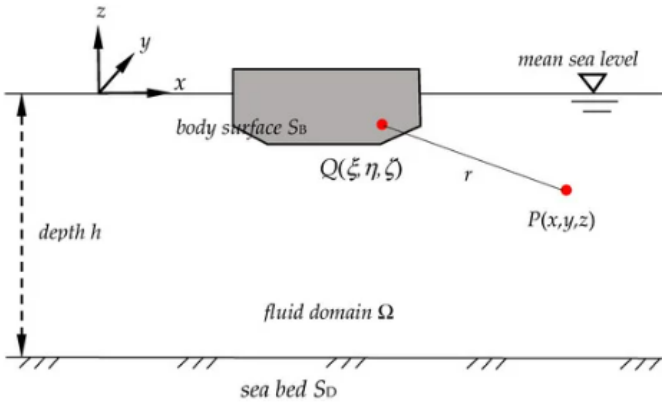


Figure 3.4: Defined coordinate system and immersed body parameters used in HAMS (Yingyi, 2019)

3.4 FAST v8.16

In this study, FAST v8.16 is used to analyze and understand the behavior of the proposed TLPWT platforms in the benchmark study. HydroDyn module of FAST is used for the hydrodynamic solution. Wave characteristics are denoted in HydroDyn module, as well as, wave kinematics as still water, regular or irregular type, significant wave height, the peak period of incident waves, heading direction of propagating wave, number of wave directions, spreading function, and second-order waves. Wave streching and higher order theories are not included in the calculation process. HydroDyn's domain of calculation is identical to that of ANSYS AQWA: the zone between the flat seabed and still water level. Within HydroDyn, waves are generated analytically at finite depth using the first order or a combination of the first and the second order wave theory (Sharma and Dean, 1981). However, this thesis

does not include implementation of second-order waves in either ANSYS AQWA or FAST because second order effects are unaffected by the stated wave period.

The potential-flow solution is applicable in HydroDyn. Frequency to time domain transformations are included in the solution process. Related hydrodynamic loads are computed with linear hyrostatic restoring, damping and added mass, linear wave radiation, Froude Krylov forces, and scattering motions and so on. Because the hydrodynamic coefficients required for the potential flow solution are frequency-based, precomputation of utilizing the frequency domain codes such as WAMIT or ANSYS AQWA is essential.

HydroDyn allows for the definition of environmental conditions (water depth, water density, gravitational acceleration), wave characteristics (kinematics, direction, wave parameters, time series, etc.), second order effects, current (using linear relationship and power law theories), and floating platform (using precomputed hydrodynamic coefficients).

When HydroDyn is coupled to FAST, HydroDyn receives the position, orientation, velocities, and accelerations of the substructure at each coupling time step. Afterwards, hydrodynamic loads are computed and returned back to FAST. At this time, FAST's ElastoDyn structural-dynamics module assumes for a floating platform that the substructure (floating platform) is a six degree-of-freedom (DOF) rigid body. Reactions, displacements and motions are computed with solution flow of FAST, and required outputs are recieved.

Additionally, the wind field is generated and controlled with AeroDyn and InFlow modules of FAST. Wind turbine aerodynamic properties are also defined within AeroDyn. Airfoils, rotor, blades, tower properties, and the influence of turbine and blades on the system are specified. The NREL MIT 5MW baseline wind turbine is implemented in FAST using NREL's ready-to-use AeroDyn code. Wind characteristics such as horizontal wind speed and reference height of horizontal wind

speed are defined in InFlow module. FAST simulation procedure and integrated modules are shown in Figure 3.5.

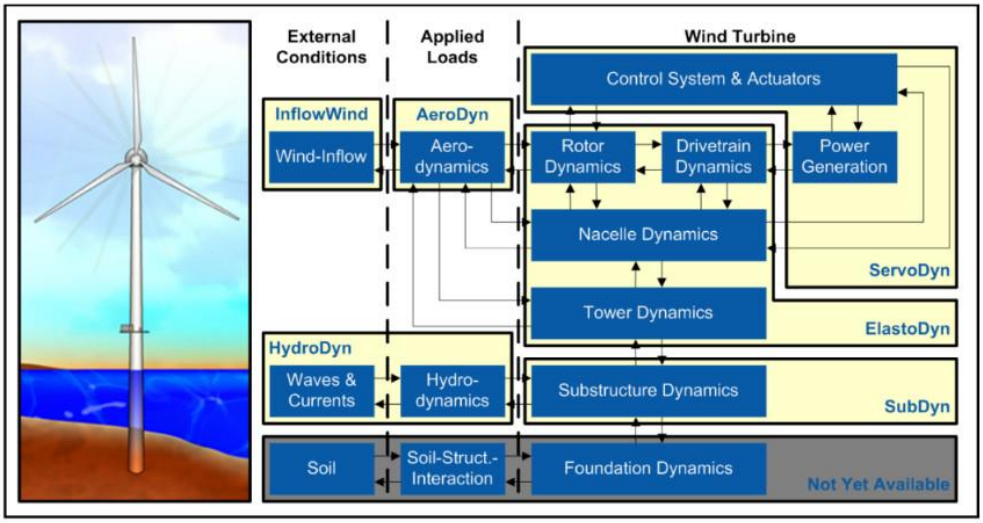


Figure 3.5: FAST Simulation Overview and Modules (Jonkman et al., 2010)

General data is compiled with the specific environment and wave propagation. FAST generates a wide variety of outputs, such as forces, displacements, and rotational motions. The data requested with the code consist of 6 DOF's and tension forces on mooring lines. Also, surge and pitch motions are referred to as critical degrees of freedom in the benchmark study , as well as the mean tendon tensions. These are estimated to guarantee that mooring system issues are resolved. Additionally, free decay tests are performed on each TLPWT model to determine the natural period of the surge motion in this thesis. Surge RAO is calculated by ANSYS AQWA, then interpreted with natural period. In terms of the aforementioned concepts, three TLP designs are compared to one another and to Bachinsky's solutions.

CHAPTER 4

NUMERICAL MODELING

This chapter discusses the three-dimensional modeling and analysis stages of designed TLPs. Throughout the aforementioned process, in Chapter 3 software and codes are presented. The geometric parameters, total masses, inertias, and other properties of TLPs, as well as the environmental circumstances used in this thesis, are identified in the following.

4.1 Geometry and 3D model

Bachinsky's defined foundations are designed to sustain a NREL 5MW turbine as a single column TLPWT with a Hywind OC3 tower and consist of three or four spokes (Jonkman, 2010, Jonkman et al., 2009, Bachinsky and Moan, 2012). The foundation's main hull is a steel cylinder that continues to a base nod where spokes are linked. Spokes are primarily responsible for transmitting dynamic loads from the mooring system to the hull. Additional wires may be necessary to improve efficiency, but these are not accounted for in the basic structural design. They are all rectangular in shape with varying diameters. At the end section, tendons are connected to spokes. Additionally, since spokes are positioned at the bottom of all foundation systems, they increase resistance to wave impact stresses via buoyancy (Matha, 2009, Kibbee, 1999).TLPWT1 has four spokes, while TLPWT2 and TLPWT3 have three spokes. TLPWT3 model representing SeaStar Oil Platform is half scaled version of the original one.

As illustrated in Figure 4.1, the geometrical properties mentioned in Bachinsky's study are as follows: D_1 and D_2 represent the diameter of the hull, h_1 represents the

length of the hull, h_p represents the height of the pontoon/spoke, w_p represents the width of the pontoon/spoke, and r_p represents the radial distance of the pontoon/spoke from the central axis of the hull. Table 4.1 summarizes the properties of TLPWTs. where n_p denotes the number of pontoons, D_t denotes the diameter of tendons, tt denotes the thickness of tendons, Z_s denotes the vertical placement of pontoons, and T_t denotes the initial tension on tendons.

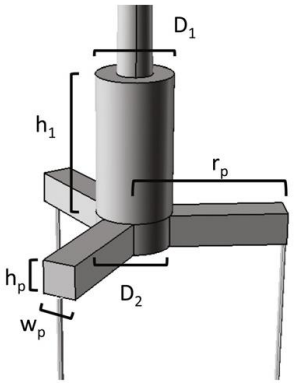


Figure 4.1: Geometrical Parameters of TLPWT Foundations (Bachinsky and Moan, 2012)

Table 4.1: Geometrical Parameters of TLPWT Foundations (Bachinsky and Moan, 2012)

PARAMETER	*TLPWT1*	*TLPWT2*	*TLPWT3*
D_1,D_2 (m)	18	14	14
h_1 (m)	51.6	40	26
h_p (m)	2.4	5	6
w_p (m)	2.4	5	6
r_p (m)	27	32	28
n_p	4	3	3

D_t (m)	1.4	1.4	1.4
tt (mm)	46.2	46.2	46.2
Z_s (m)	-43.8	-32.5	-19.00
T_t (kN)	6868	4963	8262

Using AutoCAD, 3D geometries of TLPWTs are produced in accordance with the properties listed in Table 4.1. The three-dimensional geometries of the TLPWT foundations are depicted in Figure 4.2. The origin is located in AutoCad at the hull's central axis at still water level; the 3D solid model is then exported to ANSYS AQWA with the z positive axis vertically upward and x in the upwind direction to facilitate study. Additionally, the solid-body is positioned such that the intersection point of its central axis and the center of its top surface overlaps with the origin. Due to the fact that ANSYS AQWA recognizes still water as a boundary level and operates under that elevation, importing models becomes significantly easier with this feature of the application. The above part of the foundation directly does not contribute to any hydrodynamic calculations based on the shape. However, the system incorporates the overall mass and inertia of wind turbines to obtain correct

hydrostatic and hydrodynamic findings. In addition, ANSYS AQWA defines the coordinate system as a global system by default.

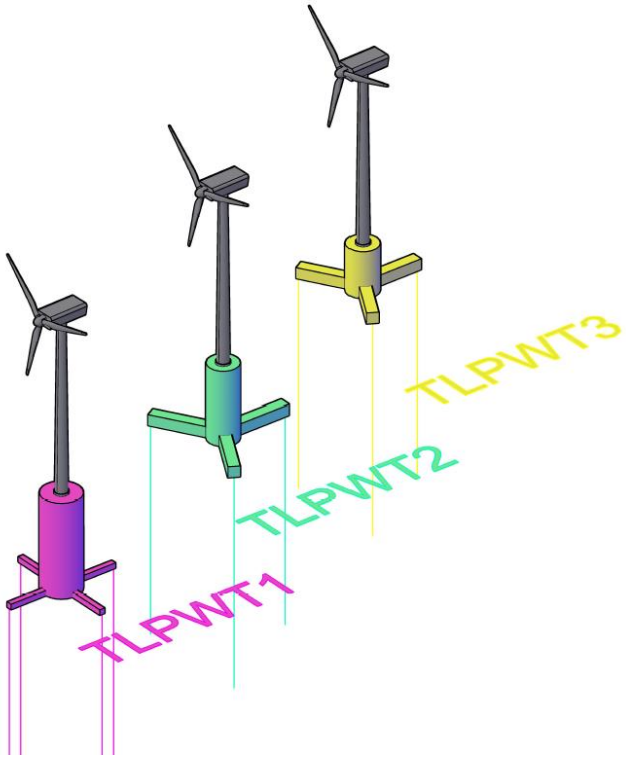


Figure 4.2: AutoCAD Models of Proposed TLPWT Foundations

Mesh of 3D solids are generated in AQWA. Methodology and theory behind the meshing capability of AQWA are explained in the ANSYS AQWA research methodology section.

The only challenge observed in meshing process performed in ANSYS AQWA may be the mesh number limitation. AQWA allows users to decide the mesh size and the number to the limit of 40000 pieces. 40000 pieces of mesh denote to 0.1m element size roughly for TLPWTs. 22500 pieces of mesh corresponds to maximum element size of 0.2m. The analysis demonstrates the convergence of meshes with 40000 and 25000 pieces. The results are not different. The mesh size has been determined to be roughly 22500. 0.2m mesh element size denotes to 0.4-0.5 percent of the hull length. As a result, the mesh size decision is appropriate to get precise results. Because of the large number of mesh components, the processing computer's central processing

unit (CPU) and graphics processing unit (GPU) are significantly overloaded. Additionally, the platforms examined in this study do not have complex geometries. The elements' smoothness facilitates processing. TLPWT1, TLPWT2, and TLPWT3 meshes generated with ANSYS AQWA are shown sequentially in Figures 4.3, 4.4, and 4.5.

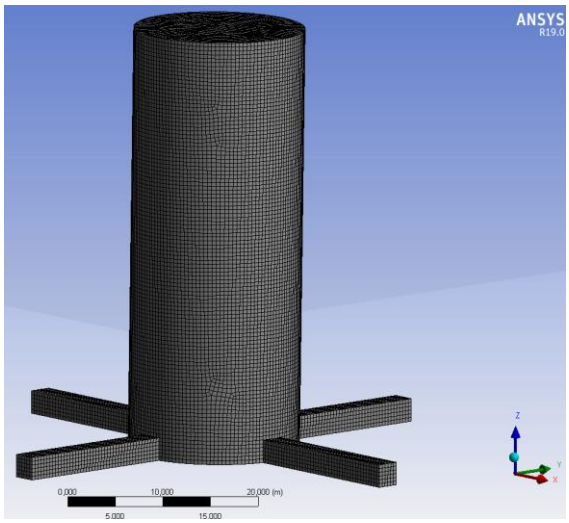


Figure 4.3: TLPWT1 Mesh Details Generated using ANSYS AQWA

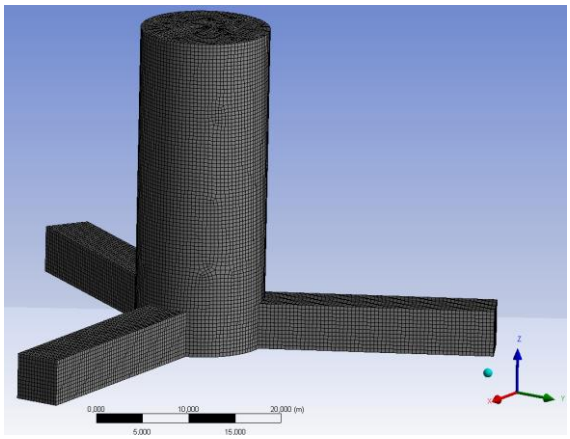


Figure 4.4: TLPWT2 Mesh Details Generated using ANSYS AQWA

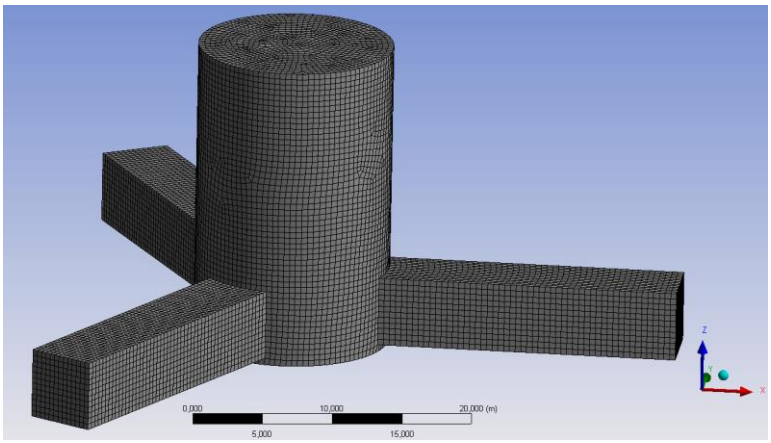


Figure 4.5: TLPWT3 Mesh Details Generated using ANSYS AQWA

FAST library contains the necessary parameters and files of frequently used baseline designs, such as NREL 5MW wind turbine. Geometries are defined in FAST using ElastoDyn, BeamDyn and ServoDyn modules. Blades and blade interfaces are implemented in ServoDyn. Turbine configurations and initial positions are determined in ElastoDyn as well as tower parameters and adjustments. BeamDyn computes the mesh, key points and tolerances related to geometry. Also, AeroDyn is responsible for advanced geometrical computations on airfoil shapes. Module files for a 5MW NREL wind turbine were mentioned in the FAST library. As a result, no changes are needed to make to the ElastoDyn, BeamDyn, or ServoDyn files. Because only the geometry of the TLP platform and mooring system differs from the baseline designs in the FAST library.

In addition, alternative HAMS solution performed to check ANSYS AQWA results includes meshing process in RHINO. The program creates dynamic mesh which means users are able to modify every mesh aspect piecewise. Also, the program checks the mesh and provide the best resolution or mesh size. In general, the program builds meshes for each of the three TLPWT models between the range of 8000 – 10000 elements. In addition, xz plane is used as symmetrical plane for the computational dynamics in HAMS shown in Figure 4.6 as an example.

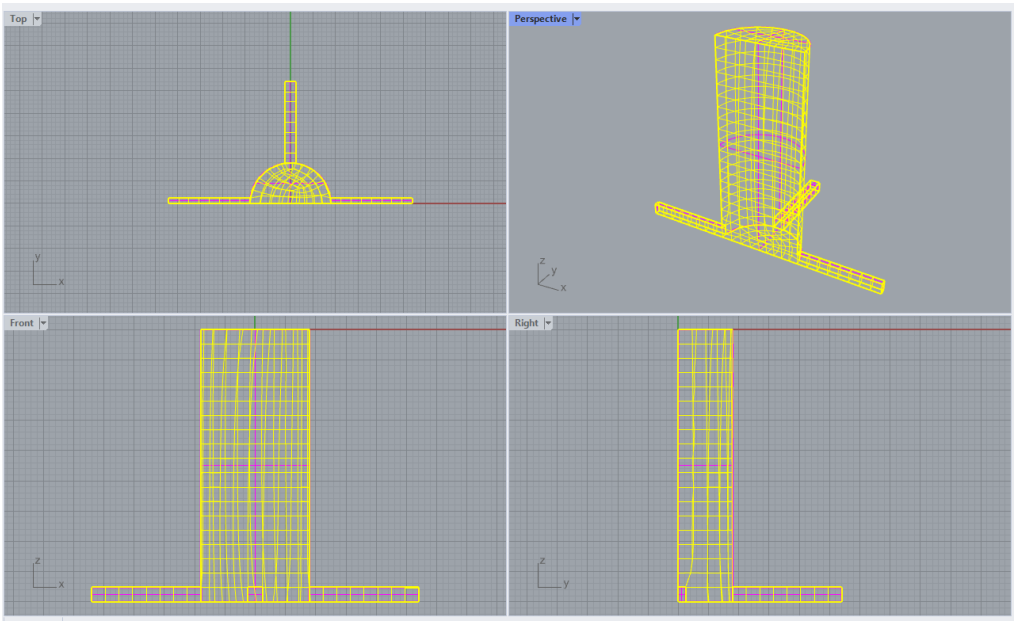


Figure 4.6: TLPWT1 Mesh Views in RHINO

4.2 Mass Properties

Geometrical parameters help to calculate the volume of different parts of the TLP foundations. Approximate steel weight values for the hull can be found in Table 4.2. They are calculated based on the assumption of steel weights per volume. Moreover, it is assumed that the steel weight is distributed uniformly throughout the body and that stokes of a specified thickness are used (Bachkinsky and Moan, 2012).

Table 4.2: Structural Steel Weight Approximations (Bachkinsky and Moan, 2012)

ELEMENT	*UNIT WEIGHT* (kg/m^3)
Column of the hull	224
Spokes	202

In AQWA, mass moment of inertias and center of masses are defined manually. Due to the availability of geometrical data, simple spreadsheet computations and formulas are sufficient. For example, mass quantities are expressed using volumetric formulations. Spokes have rectangular forms, so that the volume formula of spokes are mentioned in Equation (4.1.). Hulls have cylindrical forms, the volume is calculated using Equation (4.2). Equation (4.3) is used to calculate the masses of components based on the contribution of the particular weights listed in Table 4.2. The masses of the platform draft and spokes are calculated using a spreadsheet, while the parameters of wind turbines are gathered from related publications. In the literature, the NREL 5 MW wind turbine is frequently utilized and emulated. Table 4.3 summarizes the mass and inertia figures for wind turbine and platform components.

$$V = h_p^2 * L \quad \text{(4.1.)}$$

$$V = \frac{\pi D^2}{4} * L \quad \text{(4.2.)}$$

$$M = V * \gamma \quad \text{(4.3.)}$$

Where D denotes diameter, L denotes length and γ means unit weight.

Table 4.3: Calculated Masses and Mass Moment of Inertias of TLPWT Components

	ELEMENT	*MASS (KG)*	*MASS MOMENT OF INERTIA (kg*m²)*
TLPWT1	Draft	2565047.57	640614744.00
	Spokes	83897.87	1749269.00
TLPWT2	Draft	1206874.23	1823385815.83

	Spokes	646400.00	18179999.00
TLPWT3	Draft	793088.78	4467733460.67
	Spokes	141400.00	18179999.00
5MW NREL Turbine	Total	697460.00	36000000.00

The mass moment of inertia is a quantitative measure of a solid's rotational inertia. The parallel axis theorem is applicable to a solid body composed of fragments (Paine et al., 1994). Due to the fact that the proposed foundations consist entirely of cylindrical shapes for the draft and spokes, it is simple to implement parallel axis theory, as indicated by Equation 4.4. Moments of inertia of each component in relation to the central axes are calculated using Equation 4.5 for the draft and Equation 4.6 for the spokes. Inertias are calculated using the above formulas as a result of the geometrical components of the platform body being aligned along various centric axes. AQWA is used to make the advance computations. The inertia of a body is calculated by taking into account the contribution of each body component using the superposition principle.

$$I = I_c + M * h^2 \quad \text{.....(4.4.)}$$

$$I_c = \frac{1}{2} M * R^2 \quad \text{.....(4.5.)}$$

$$I_c = \frac{1}{4} M * R^2 + \frac{1}{12} M * L^2 \quad \text{.....(4.6.)}$$

Where I_c denotes the inertia along the central axis, R denotes the radius, and I is the total inertia.

Gravitational acceleration and seawater density are assumed to be universally accepted values of 9,80665 m/s^2 and 1025 kg/m^3, respectively.

On the other hand, the baseline designs are specified in FAST with associated files. NREL 5MW wind turbine can be identified in a FAST progress with ElastoDyn and ServoDyn modules. Wind turbine components such as rotor, hub, tower etc., are implemented into the system using ElastoDyn in terms of masses and inertias. ServoDyn is used to control the generator torque and nacelle movements. TLP platform and mooring system behaviors that are mass and inertia dependent are defined in the FAST system using the HydroDyn module.

4.3 Mooring System

TLPWT designs modeled in this study have approximately the same mooring system as the benchmark case. Tethers and tendons have the same properties. However, spoke numbers of the platforms are different. TLPWT1 and TLPWT2 designs are inspired by Matha's thesis. TLPWT1 is an actual design that Matha proposed (Matha, 2009). TLPWT2 is the modified version in terms of hull mass properties. Tendon arrangements are modified and simplified accordingly to satisfy mooring requirements in Bachinsky's study. The original design has four tendons whereas Bachinsky uses eight tendons. In this thesis, Bachinsky is accepted as the reference study. Eight tendons are used for TLPWT1 and six tendons are used for TLPWT2, TLPWT3 in this thesis. Bachinsky's analysis found no difference in the mooring system between TLPWT1 and TLPWT2. Moreover, the mooring system is approximated and simplified by always assuming straight tendon lines regardless of wave movement.

Table 4.4: Mooring System Properties of Modeled TLPWT's (Matha, 2009)

PROPERTIES	*VALUE*
Number of mooring lines	4

Line diameter (m)	0.127
Steel wall thickness (m)	0.015
Line extensional stiffness (N)	1500000000

Mooring tendons supposed to be hollow circular pipes. At the final point, it is decided to fictionalize the mooring system as two tendon for each pontoon (Bachisnky and Moan, 2012).

The benchmark study is adjusted from a cost-effectiveness standpoint. However, this thesis makes no mention of the cost-benefit analysis. Tendon properties such as extensional stiffness, diameter and thickness determined in accordance with Figure 4.4. Tendons, on the other hand, are supposed to have zero weight in water. Thus, with typical steel calculations, thickness (tt) becomes 0,033 of diameter (D_t) of tendons in order to satisfy this requirement (Matha, 2009). The work and modeling in this thesis are based on Matha's 2009 study.

The FAST code includes the FEAMooring module, which is used to define the mooring system. The parameters tabulated in Table 4.4. are used as the input for FEAMooring. Tendons are numerically located in the code in relation to the parameters indicated in Figure 4.7. on a cylindrical hull, where LAngAnch is the angle of the anchor point (deg), LAngFair is the angle of the fairlead point (deg), and LRadAnch is the radius of the anchor point (m). Additionally, as indicated in Table 4.1., initial tendon tensions (T_t) are defined for each TLPWT design.

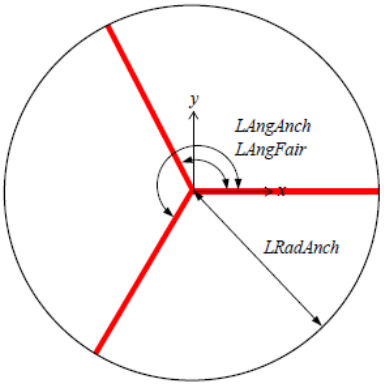


Figure 4.7: Mooring Line Location Parameters (NREL, 2009)

4.4 Environmental Conditions

TLPWT foundation types vary mostly in response to water depth. TLP solutions are often considered to be in the range of 70m to 200m. This study and the benchmark study are conducted for a water depth of 150m (Bachinsky and Moan, 2012).

TLPWT's will be tested in directional uniform wind and irregular wave conditions. As illustrated in Table 4.5, the benchmark study compares the designs in six distinct environmental scenarios (Bachinsky and Moan, 2012). However, the cases with the highest wave height, the longest period, and the strongest wind are designated as Condition 4 and 5 in Table 4.5 for this study. Because the most critical coupling impact reveals the most significant difference among the platforms. However, wind forces dominate the system under condition 4 due to the high wind speed (50 m/s), and hydrodynamic effects are not observed clearly. For this study, condition 5 is chosen. 12.7 m and 14.1 sec are chosen as the significant wave height and peak period, respectively. The mean wind speed at the hub is taken to be 18 m/sec.

Table 4.5: Environmental Conditions (Bachinsky and Moan, 2012)

CONDITION		*1*	*2*	*3*	*4*	*5*	*6*
Significant Wave Height (H_s)	m	2.5	3.1	4.4	12.7	12.7	3.1
Peak Wave Period (T_p)	s	9.8	10.1	10.6	14.1	14.1	10.1
Mean Wind Speed (U)	m/s	8	11.4	18	50	18	12

All TLPWTs are subjected to the identical wave and wind condition, and the results are compared because the primary objective of this study is to compare the geometries of different TLPWT foundations utilizing various programs from Baschinsky's work. The environment should be identical for all TLPWTs in order to verify that the outcomes are determined solely by geometrical parameters.

The simulated wave series are utilized as the JONSWAP spectrum to demonstrate how crucial enhancement factors are influenced by substantial wave height and peak duration (MARINTEK, 2011). Additionally, when the period is large and the interval time is low, the period interval number increases to ensure that codes operate precisely. 0.0125 seconds is determined as the interval time in 60 minutes. For more realistic scenarios, a larger time margin can be considered. The directions of the wind and waves are regarded to be aligned. Finally, the second-order effects of wave dynamics are ignored. A wave with a fixed period does not generate significant movement in the same way as waves with longer durations do in primary situations, such as tsunamis. Therefore, the effect of secondary order is insignificant.

HydroDyn and InFlowWind modules define the environmental conditions in FAST. HydroDyn module includes wave parameters such as wave height, period, direction, kinematic features, and second-order effects. This module also incorporates hydrodynamic coefficients into the FAST system. The InFlowWind module demonstrates wind characteristics such as kinematics, speed, direction, and reference height for specified speed and direction.

Simplifications of parameters and environmental conditions are done for each of the three TLP designs in order to maintain the basic comparison purpose. Through software and codes, geometry, mass, and tendon properties are simplified and made more processable. Another advantage of this approach is that it avoids data adaptation problems between modeling software and simulation code by describing attributes as simply as feasible because the procedure and data need to be easily recognized by FAST.

CHAPTER 5

RESULTS

This chapter summarizes the findings. Each TLPWT design is evaluated in comparison to the others. Additionally, differences between the benchmark study and this thesis are highlighted. To demonstrate the effects of geometrical parameters, various TLPWT designs are modeled and analyzed in the same environment.

The most often used coupled TLP analysis procedure necessitates the usage of different codes. Multiple software or open source codes are utilized to interpret the hydrodynamic behavior of TLPWT.

Hydrodynamic coefficients are calculated using ANSYS AQWA software and HAMS. Wind and wave conditions are taken as homogeneous and unidirectional, in this study. For TLPs, motions in pitch and surge directions are crucial. The change in the natural frequency of surge as a result of the coupling mode between surge and pitch may jeopardize the system's stability. Turbulent conditions may result in different yaw and roll motions, however the turbulent flow is not considered in this thesis. Following the benchmark case, wind and wave are considered as uniform.

The platform tends to behave in a high-frequency range in terms of resonance in restricted modes. The design of the mooring system has two critical limiting conditions. The first is when a mooring line snaps, resulting in destabilization. The other issue is slacking, which occurs when tension in the mooring line is lost. The mean tendon tension provides context for assessing the probability of a slacking problem. RAOs and associated natural frequencies should not overlap. If, RAOs and natural frequencies coincides with each other, this situation may result in resonance phenomena. It means, there will be destruction in TLP system.

Bachinsky’s reference paper solves TLPs’ aero-hydro-servo problem with the conventional method that includes SIMO, RIFLEX, WAMIT and FAST process. In addition, spreadsheet calculations are performed to validate results and evaluate natural frequencies. In this thesis, the hydrodynamic behavior of TLPs is solved through the use of ANSYS AQWA software and HAMS. The coupling analysis of TLP is carried out with FAST. Free decay tests are carried out and following this natural frequencies and RAOs are checked to understand whether there is a resonance behavior.

5.1 General Comparison

Visualization is critical for realizing the behavior, motions, displacements, and responses of a system. ANSYS AQWA enables users to simulate and visualize three-dimensional dynamic motions. The benchmark study provides extensive information regarding the geometries of TLPWTs, which can be viewed as a benefit for the advancement of 3D modeling, which requires precise measurements to generate a solid model. ANSYS AQWA makes it simple to model hull and pontoon shapes. Modeling mooring systems in ANSYS AQWA is challenging, because the materials used to manufacture pontoons, tendons, anchors, and connections should be characterized by their stiffness, young's modulus, and stiffness coefficients, among other properties. Additionally, their location should be carefully determined by considering diameters, thicknesses, and other dimensions, as precise coordinates are necessary for connections, and incorrectly supplied attributes can result in problems. In this thesis, ANSYS AQWA is used only to obtain hydrodynamic coefficients. FAST modules are used to integrate a mooring system and wind turbine into the system.

The ANSYS AQWA results of this study are listed in Table 5.1 as mean values, while Bachinsky's are tabulated in Table 5.2.

Table 5.1: Mean Values of Surge, Pitch, Tendon Tension Ratio and Surge RAO Calculated in This Study with ANSYS AQWA

PROPERTIES	*TLPWT1*	*TLPWT2*	*TLPWT3*
Surge (m)	2.472	3.332	2.620
Pitch (deg)	0.0078	0.015	0.017
Tendon Tension Ratio (-)	0.880	0.934	0.980

Table 5.2: Mean Values of Surge, Pitch, Tendon Tension Ratio Calculated in Bachinsky's Study (2012)

PROPERTIES	*TLPWT1*	*TLPWT2*	*TLPWT3*
Surge (m)	2.200	3.000	2.500
Pitch (deg)	0.006	0.010	0.010
Tendon Tension Ratio	0.800	0.800	0.850

Results for surge and pitch motions are similar between the benchmark study and this thesis as can be seen in Table 5.1 and 5.2. A slight difference is observed between the same parameter values. Results of this thesis have barely higher value than the benchmark study. The reasons for that may be rounding errors while transforming the outputs used in the process and may be CAD programs used in this thesis that may have high factor of safeties in the solution process. Also, the general view demonstrate that surge becomes more critical than pitch motion, due to the fact that, the pitch motion difference is negligible than the difference in surge observed between TLPWT1, 2 and 3. The surge motions are mainly caused by the wind which is the same for all designs. However, environmental conditions are same for TLPWTs. Thus, the systems' geometry and mass cause the difference between TLPWT designs. The draft height and mass are decreased from TLPWT1 to TLPWT3. Also, a TLPWT system becomes vulnerable to motion in an aligned direction with the wind and wave. The wave and wind are exerted on TLPWTs in surge direction (+x axis).

5.2 Surge Natural Periods and Surge RAO

Free decay tests can be used to determine a system's natural period. Resonance condition of the system can be eliminated with the comparison between system's natural period and related motion's RAO. The natural period and RAO should be different.

When carrying out free decay test in surge directioın, a minor displacement is applied to the system in a still environment (free of wind and wave). The oscillations are followed until the system reverts to its original position. Generally, the initial displacement amount has no effect on the system's response.

Table 5.3: Natural Periods and Surge RAOs of the Models

	PROPERTIES	*TLPWT1*	*TLPWT2*	*TLPWT3*
Bachinsky	Surge Natural Period (sec)	57.00	55.00	45.00.
FAST	Surge Natural Period (sec)	56.27	52.26	41.86
ANSYS AQWA	Surge RAO Period (m/m)	14.10	10.03	7.79

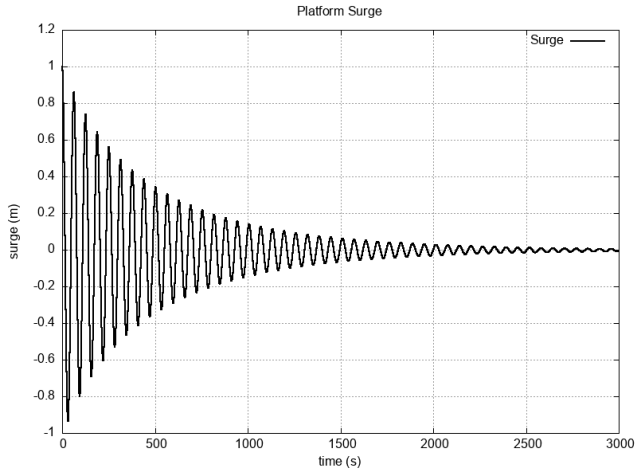


Figure 5.1: Free Decay Test Graph of TLPWT1 (FAST)

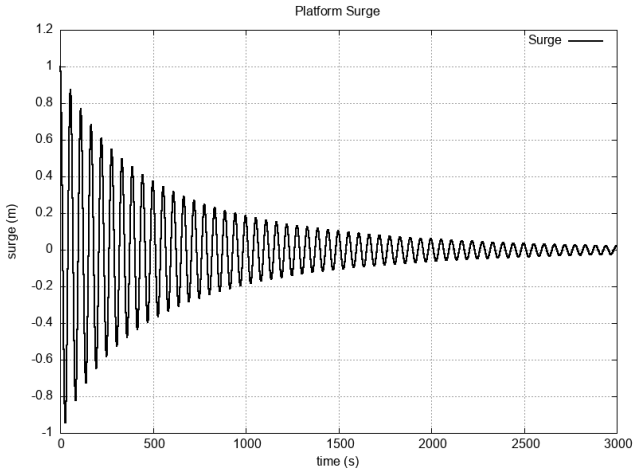


Figure 5.2: Free Decay Test Graph of TLPWT2 (FAST)

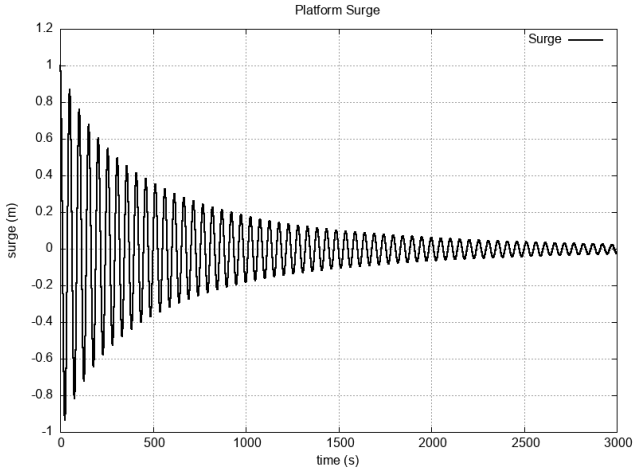


Figure 5.3: Free Decay Test Graph of TLPWT3 (FAST)

All free decay tests in surge motion are carried out for 3000 sec simulation duration and initial displacement is given as 1m, in FAST. The test is conducted over an extended period of time in order to observe total attenuation, as illustrated in Figures 5.1, 5.2, and 5.3. The test period is shortened in order to clearly acquire natural periods. The trials demonstrate that a 100-second test time is optimal for obtaining natural periods. In Figure 5.4, 5.5, and 5.6, free decay test graphs clearly demonstrate the natural periods of TLPWTs.

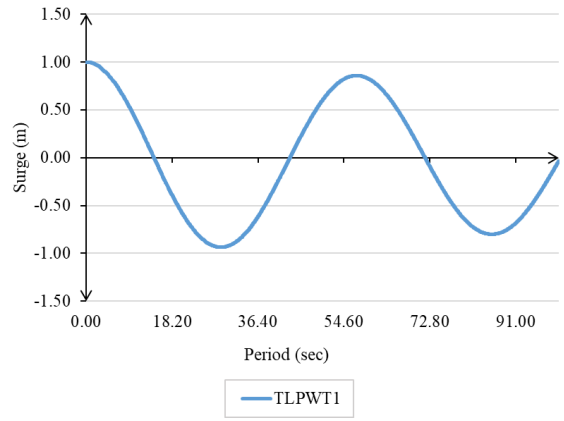


Figure 5.4: Free Decay Test Graph of TLPWT1 (FAST)

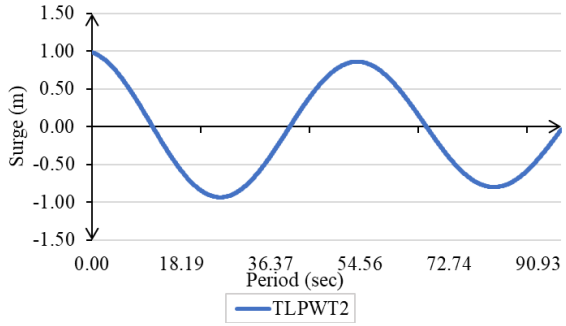


Figure 5.5: Free Decay Test Graph of TLPWT2 (FAST)

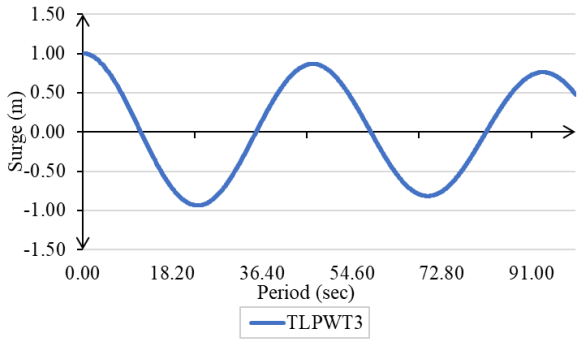


Figure 5.6:Free Decay Test Graph of TLPWT3 (FAST)

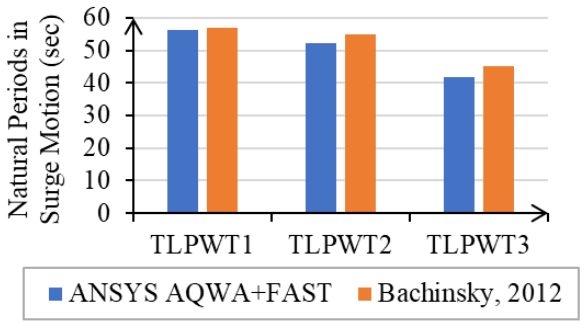


Figure 5.7: Natural Periods of TLPWTs in Surge

On the other hand, the reference study generates natural periods for proposed designs in surge motion utilizing free decay tests and a comprehensive finite element model (Bachinsky, 2012). As illustrated in Figure 5.7, there is a slight difference between the obtained and represented periods in the reference study. TLPWT1 has a longer natural period than TLPWT3, as an increase in hull volume corresponds to an increase in natural period.

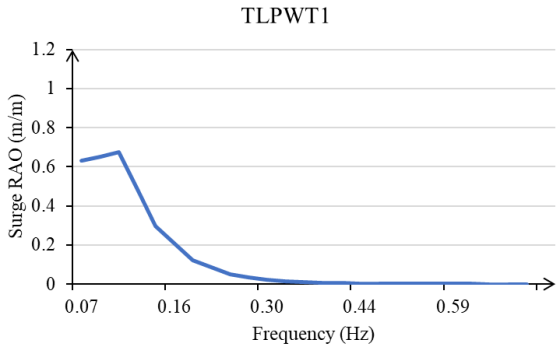


Figure 5.8: Surge RAO Graph of TLPWT1 (from ANSYS AQWA)

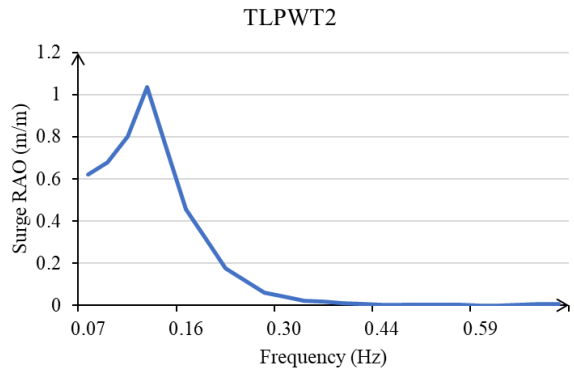


Figure 5.9: Surge RAO Graph of TLPWT2 (from ANSYS AQWA)

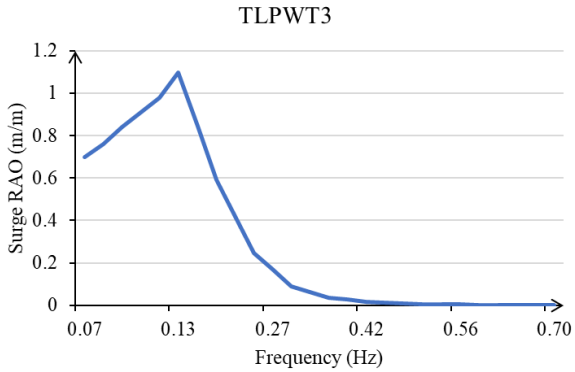


Figure 5.10: Surge RAO Graph of TLPWT3 (from ANSYS AQWA)

The surge RAO is calculated in this work using ANSYS AQWA, and the frequency at which the surge RAO reaches its peak is designated in Table 5.3. In Figures 5.8, 5.9, and 5.10, related graphs depict the corresponding frequency value for the peak surge value. For each of the TLPWT designs, the RAOs are shorter than the natural periods determined using free decay tests, as shown in Table 5.1. Moreover, the pitch and surge responses calculated in this study are only slightly greater than those estimated in Bachinsky's study.

5.3 Surge and Pitch Motions

Graphwise and data-to-data comparison could not be carried out between the benchmark study and this thesis. Because, calculated data set in the benchmark study

is not publicly available. At this point, HAMS results obtained in this thesis are taken into consideration. Findings of ANSYS AQWA work flow is compared with HAMS in order to ensure reliability of matching results with the benchmark study. Surge and pitch motions of TLPWTs analyzed in this study with (ANSYS AQWA + FAST) and (HAMS + FAST) are shown in Figure 5.11. and 5.12.

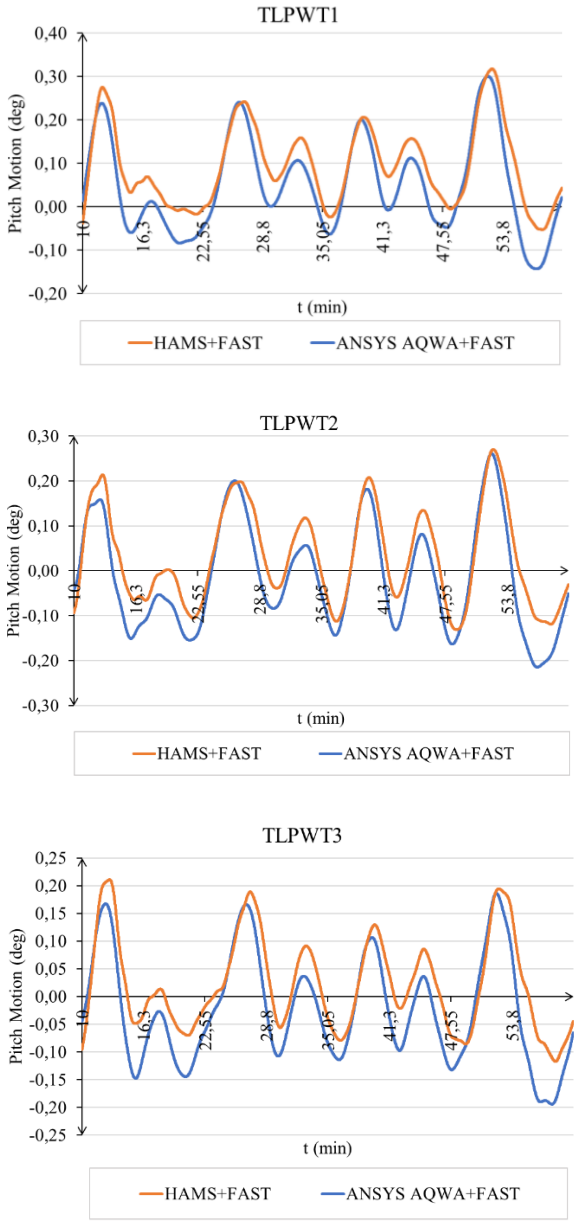


Figure 5.11: Pitch Motions of TLPWTs

Simulation duration is taken as 60 minutes. However, results of the analysis at the first 10 minutes may be inconsistent. Therefore, all of the graphs do not include the results of the first 10 minutes of the analysis.

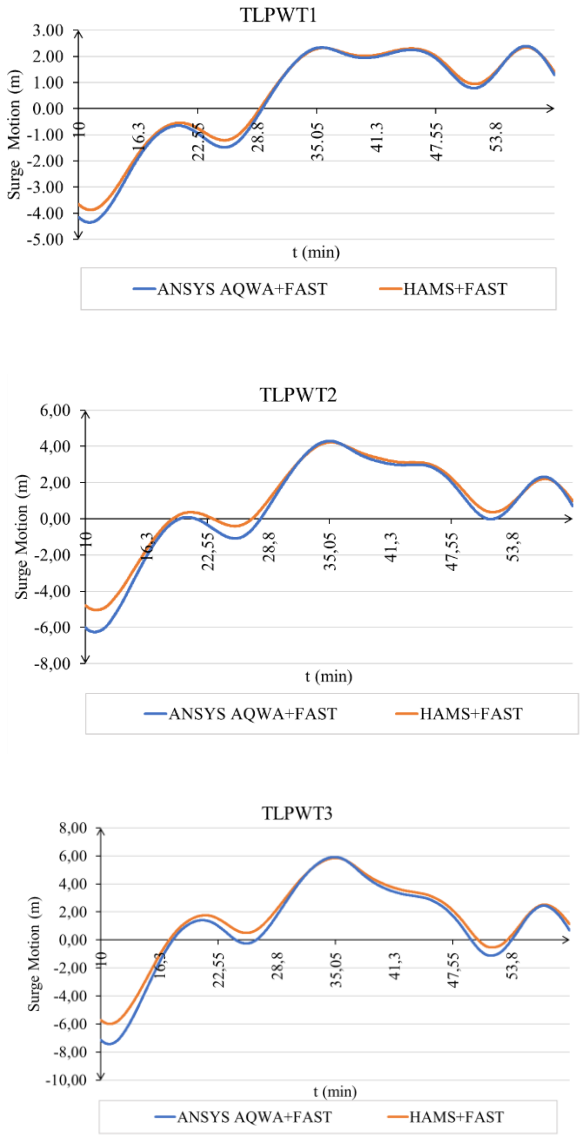


Figure 5.12: Surge Motions of TLPWTs

In general, pitch and surge motions are observed as similar in (ANSYS AQWA + FAST) and (HAMS + FAST). Although pitch motion findings obtained from (HAMS + FAST) and (ANSYS AQWA + FAST) are almost equal, surge motions have small differences. However, the maximum surge values are the same as can be seen in

Figure 5.12. In mean value comparison, the differences between (ANSYS AQWA + FAST) and (HAMS + FAST) can be seen clearly in Figure 5.13 and 5.14. But, the overall findings are negligibly different from each other.

ANSYS AQWA model consists of only hull, pontoons, and wave interaction with element masses without any limiting elements. Turbine mass is added for more accurate results in terms of moments and inertias. FAST is used to solve the TLPWT system following the hydrodynamic analysis. Additionally, there may be differences in the rounding of numbers and assumptions. Thus, the results of the reference study elucidate more restricted motions in terms of surge and pitch than the solutions given in this study.

Pitch has a greater effect on tendon tension than surge, because the increase in tendon tension caused by surge motion is typically less than the decrease caused by pitch (Bachinsky, 2012). Although surge response is not crucial for tendons, tendon angles can be considerable at sea bottom connections or attached submerged platform connections as a result of surge motion. The pitch angle changes as the tower height, draft depth, or wave height increases. Due to the fact that the pitch amplitude is not detected beyond 1 degree, it is not a critical constraint for the designs depicted in Figure 5.14. Additionally, the TLPWT3 exhibits the most pronounced pitch according to (ANSYS AQWA + FAST), as evidenced by the difference between the reference study and this research. The smallest hull may be more prone to rotational motions than bigger hulled devices.

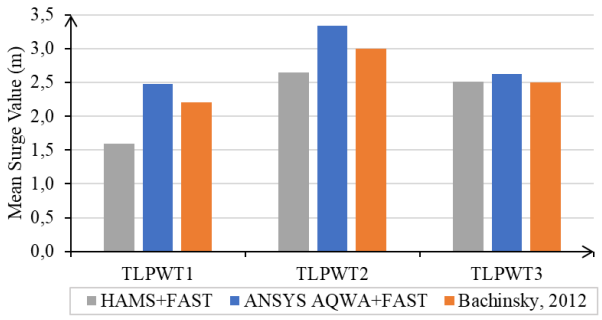


Figure 5.13: Mean Surge Responses of TLPWTs

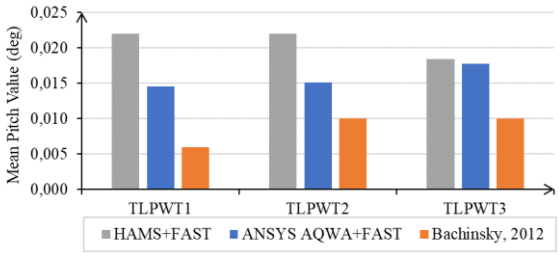


Figure 5.14: Mean Pitch Responses of TLPWTs

5.4 Tendon Tensions

Tendon failure probability can be estimated using a straightforward method called the safety factor, as introduced by Bachinsky. The mean tendon tension values computed via FAST are divided into the initial tensions in mooring lines. The cross-sectional area of the tendon should be sufficient to prevent steel tendon yielding. The chosen safety factor is twice the initial tension (Bachinsky, 2012). The results demonstrate that line breaking or slacking difficulties are not observed, as illustrated in Figure 5.15.

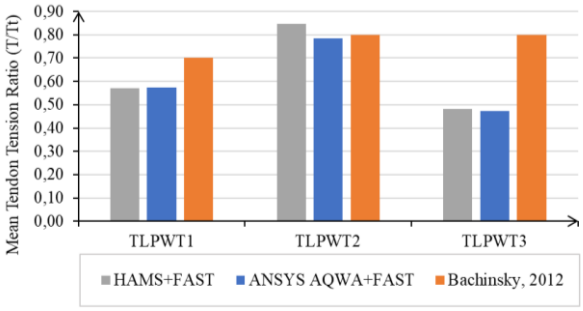
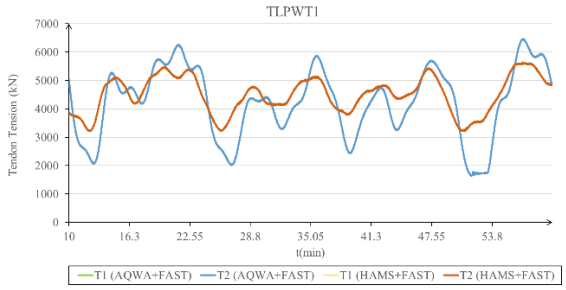


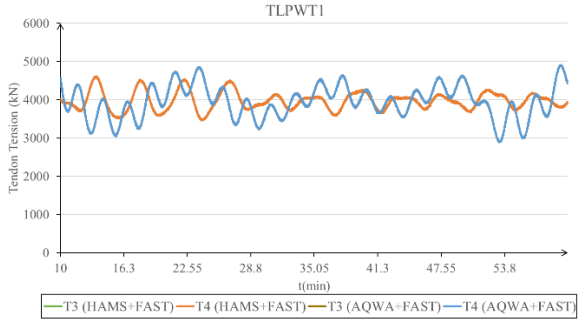
Figure 5.15: Mooring Lines Ratios of TLPWTs

Additionally, the calculated ratios in this study are smaller than the ratios indicated in the reference study. However, the ratios are based on mean values. General view of tendon tension graphs may indicate clear perspective that the system is more restricted in the (HAMS + FAST) solution. In addition to previous discussions, (HAMS + FAST) results show tendon tension range difference more clearly. Altough the mean tendon tensions calculated with (ANSYS AQWA + FAST) work flow are

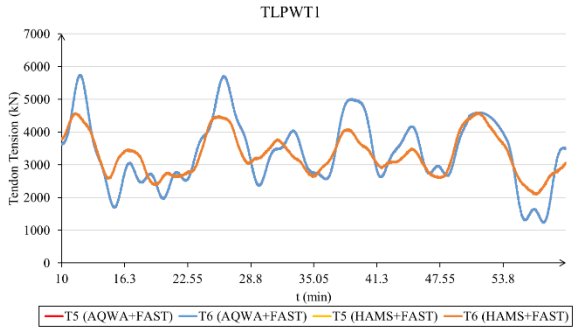
similar to those specified in the benchmark study, the maximum and minimum tension values are quite different from (HAMS + FAST) results.



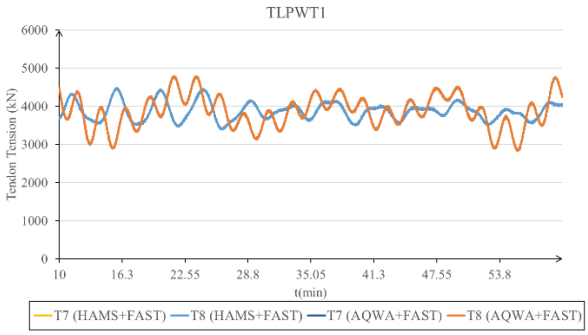
(a)



(b)



(c)



(d)

Figure 5.16: Tendon Pairs of TLPWT1 - (a):T1-T2, (b):T3-T4, (c):T5-T6, (d):T7-T8

TLPWT1 has four spokes with eight tendons, in total. Tendons are attached to each spoke as pairs. T1-T2, T3-T4, T5-T6 and T7-T8 are the tendon pairs. On the other hand, TLPWT2 and TLPWT3 have three spokes with six tendons attached. Thus, their tendon pairs are T1-T2, T3-T4, T5-T6. Time series graphs of tendon tensions of TLPWT1 are shown in Figure 5.16 as an example.

Moreover, (ANSYS AQWA + FAST) and (HAMS + FAST) graphs can be considered as evidences that slacking problem is not a concern. Because, none of the tendons lose its tension. Also, pairs work together. However, the difference in tension between opposing tendons is higher in (ANSYS AQWA + FAST) solution than (HAMS + FAST). Assumptions and calculations performed in (HAMS + FAST) may be more convinient than (ANSYS AQWA + FAST) for other structures.

CHAPTER 6

SUMMARY AND CONCLUSION

The TLP concept is frequently preferred due to its favorable stabilization responses and ease of installation. However, the design phase could be challenging due to its multidisciplinary nature. Numerous models and comprehensive tool options are available for designing and analyzing TLP structures. Additionally, researchers propose efficient platform designs that overcome aero-hydro-servo loads as much as possible. FAST and related codes are mostly used to understand the behavior of TLPs in response to specific wave and wind conditions.

The main aim of this study is to carry out a numerical analysis of a TLP using two different hydrodynamic program (ANSYS AQWA and HAMS) rather than commonly used tools (WAMIT, SIMO, RIFLEX) mentioned in a benchmark study (Bachinsky, 2012). Available software at METU, which is ANSYS AQWA, is used to prepare 3D models of TLPs and to demonstrate visuals for the analysis process, to present the results obtained from hydrodynamic analysis. Moreover, results of this thesis are compared with the results of the benchmark study.

Three TLPWT designs are modeled and analyzed in this thesis. The related hydrodynamic coefficients are compared to those in the reference work that analyzes TLPWT designs (Bachinsky, 2012). The study flow begins with a solid drawing in AutoCAD, followed by hydrodynamic modeling and analysis (i.ANSYS AQWA, ii.HAMS) and finally, coupled analysis using FAST.

Because the benchmark study had clear data about surge, pitch, tendon tensions and natural period, these parameters are investigated. The findings of the two analysis ,which are the benchmark study and process through this thesis, demonstrate a high degree of compatibility. The outcomes can be listed as follows;

- Surge and pitch motions become more restrained while the structure becomes greater. The benchmark study shows less motions in surge and pitch motions.
- Free decay tests are carried out with FAST to obtain natural period of surge motion. Related RAO is computed with ANSYS AQWA. In the benchmark study, natural periods are calculated with spreadsheet. Obtained results for natural period are agreed with the benchmark study.
- The values of natural period and RAO are not the same and do not overlap. As a result, it is decided that resonance is not a concern for the modeled TLPWTs.

The results of the (ANSYS AQWA + FAST) solution demonstrate slightly higher motions than the benchmark study. Tension results of (ANSYS AQWA + FAST) becomes slightly higher than (HAMS + FAST) findings.

This study shows that ANSYS AQWA and HAMS ,which are hydrodynamic solvers, are applicable and convenient for someone who is just learning the TLPWT concept. Subsequently, the applicability and reliability of a software, ANSYS AQWA, and the procedure are compared with results which are mentioned in the benchmark study. Since (HAMS + FAST) and (AQWA + FAST) perform similarly, ANSYS AQWA can be used in the coupled analysis of TLPWTs. And also, the results show that HAMS can be used instead of WAMIT, in hydrodynamic analysis of TLPWTs. By doing that, the dependency of WAMIT in FAST analysis may be eliminated with HAMS which is an open source code.

The mooring system was not defined effectively in ANSYS AQWA, in this study. Therefore, present work carried out in this thesis may be extended by modeling mooring system using ORCAFLEX. Because, a detailed tethers or catenaries can provide additional reliable inputs for FAST. Moreover, other offshore wind turbine platforms such as spars should be analyzed with (ANSYS AQWA + FAST) to ensure applicability of ANSYS AQWA to offshore floating wind turbine’s coupled analysis, not only vessels.

REFERENCES

ANSYS, (2016), AQWA Theory Manual

Afsharzade, N.; Papzan, A.; Ashjaee, M.; Delangizan, S.; Van Passel, S.; Azadi, H. (2016), Renewable energy development in rural areas of Iran. Renew. Sustain. Energy Rev. 65, 743–755.

Alkarem, Y., Aktaş, K., Ozbahceci, B. (2018). Açık Deniz Rüzgar Türbinleri Yüzer Platformlarinin Hidrodinamik Modellenmesi, 9. Kıyı Mühendisliği Sempozyumu, Turkey.

Bachynski, E., Moan, T. (2012). Design considerations for tension leg platform wind turbines. Marine Structures, 29(1), 89–114. https://doi.org/10.1016/j.marstruc.2012.09.001

Bachynski, E. , Moan, T. (2012). Linear and nonlinear analysis of tension leg platform wind turbines. In: The 22nd international ocean and polar engineering conference, no. 2012-TPC-0629.

Bak, C., Zahle, F., Bitsche, R., Taeseong, K., Yde, A., Henriksen, L.C., Natarajan, A., Hansen, M.H., (2013). Description of the DTU 10 MW Reference Wind Turbine. https://doi.org/10.1017/CBO9781107415324.004. Report-I-0092.

Bhaskara Rao, D. S., Panneer Selvam, R., Srinivasan, N. (2012). Hydrodynamic analysis of Tension Based Tension Leg Platform. Proceedings of the International Conference on Offshore Mechanics and Arctic Engineering - OMAE, 1, 201–207. https://doi.org/10.1115/OMAE2012-83256

Brennan, F.P., Falzarano, J., Geo, Z., Lendet, E., Le Boulluec, M., Rim, C.W., Sirkar, J., Sun, L., Suzuki, H., Thiry, A., Trarieux, F., Wang, C.M., (2012). Offshore renewable energy. In: International Ship and Offshore Structures Congress (ISSC). pp. 153–200. Rostock/Germany.

Butterfield, S., Musial, W., Jonkman, J., Sclavounous, P. and Wayman, L.. (2005). Engineering challenges for floating offshore wind turbines. Copenhagen offshore wind conference, no. NREL/CP-500-38776.

Castro-Santos, L., Martins, E., Guedes Soares, C. (2017). Economic comparison of technological alternatives to harness offshore wind and wave energies. Energy, Elsevier, vol. 140(P1), pages 1121-1130.

Cekirdekci, B.T., (2015). CFD Applıcatıons For Seakeepıng Calculatıons Of Floating Bodies. MSc. Thesis.

Chakrabarti S.K., Hanna S.Y.. (1990). Added mass and damping of a TLP column model. In: Offshore technology conference, no. OTC 6406; p. 559–71.

Costabel, M. (1987). Principles of boundary element methods. Computer Physics Reports, 6(1), 243–274.

DNV, GL. (2019). DNVGL-RP-0286 Coupled Analysis of Floating Wind Turbines.

Erdozain, J. O. (2019). Advanced Control for Floating Offshore Wind Turbines. Doctoral Thesis.

Falcao AF de O. (2010). Wave energy utilization: a review of the technologies. Renewable and Sustainable Energy Reviews, 14:899-918.

Faltinsen O. (1990). Sea loads on ships and offshore structures. Cambridge University Press.

Gareiou, Z., Drimili, E., & Zervas, E. (2020). Acceptance Of Renewable Energy Sources. Low Carbon Energy Technologies in Sustainable Energy Systems (pp. 309–327). Academic Press.

Henderson, A.R., Argyriadis, K., Nichos, J. and Langston, D.. (2010). Offshore wind turbines on TLPs – assessment of floating support structures for offshore wind farms in German waters. In: 10th German wind energy conference, Bremen, Germany.

IRENA, (2019). Future of wind: Deployment, investment, technology, grid integration and socio-economic aspects (A Global Energy Transformation paper), International Renewable Energy Agency, Abu Dhabi.

Jain AK. (1997). Nonlinear coupled response of offshore tension leg platforms to regular wave forces. Ocean Engineering ; 24(7):577–92.

Jeon, M., Lee, S., Lee, S., (2014). Unsteady aerodynamics of offshore floating wind turbines in platform pitching motion using vortex lattice method. Renew. Energy 65, 207–212. Jonkman, J., Butterfield, S., Musial, W., Scott, G., 2009.

Jonkman, J. (2007). Dynamics Modeling and Loads Analysis of an Offshore Floating Wind Turbine. NREL/TP-500-41958. Golden, CO: National Renewable Energy Laboratory.

Jonkman, J., Butterfield, S., Musial, W. and Scott, G. (2009). Definition of a 5-MW reference wind turbine for offshore system development. Tech. rep. NREL/TP-500-38060. National Renewable Energy Laboratory.

Jonkman, J. (2010). Definition of the floating system for Phase IV of OC3. Tech. rep. NREL/TLP-500-47535.

Jonkman, B. J. and Jonkman, J. M.. (2016). “FAST v8.16.00a-bjj,” tech. rep., NREL.

Jonkman B. (2009). TurbSim user’s guide: version 1.50. Tech. rep. NREL/TP-500-46198. National Renewable Energy Laboratory.

Kausche, M., Adam, F., Dahlhaus, F., & Großmann, J. (2018). Floating offshore wind - Economic and ecological challenges of a TLP solution. Renewable Energy, 126, 270–280. https://doi.org/10.1016/j.renene.2018.03.058

Kibbee, S.E, Leverette, S.J., Davies, K.B. and Matten, R.B. (1999). Morpeth SeaStar mini-TLP. In: Offshore technology conference, no. OTC 10855.

Lee, K. H. (2005). Responses of Floating Wind Turbines to Wind and Wave Excitation. MSc Thesis. University of Michigan.

Lopez, I., Andreu, J., Ceballos, S., Martínez de Alegría, I., Kortabarria, I.. (2013). Review of wave energy technologies and the necessary power-equipment. Renew Sustain Energy Rev. 27:413-34.

Maradin, D. (2021). Advantages And Disadvantages Of Renewable Energy Sources Utilization. International Journal of Energy Economics and Policy, 11(3), 176–183. https://doi.org/10.32479/ijeep.11027

MARINTEK. (2011). SIMO user's manual.

MARINTEK. (2011). RIFLEX user's manual.

NREL, (2009). FEAM Dynamic Mooring Module User's Guide.

Matha, D. (2009). Model development and loads analysis of an offshore wind turbine on a tension leg platform, with a comparison to other floating turbine concepts. Master's thesis. University of Colorado-Boulder.

Matha, D., Fischer, T., Kuhn, M., Jonkman, J.. (2010). Model development and loads analysis of a wind turbine on a floating offshore tension leg platform. no. NREL/CP-500-46725.

Moriarty, P.J., Hansen, A.C.. (2005). AeroDyn theory manual. Tech. rep. NREL/TP-500-36881.

Oguz, E., Akgul, M.A., İncecik, A. (2013). Offshore wind farms: Potential and applicability in the Southern Marmara Region, Turkey. In: 15th International Congress of the International Maritime Association of the Mediterranean (IMAM), Developments in Maritime Transportation and Exploitation of Sea Resources. Guedes Soares & López Peña (eds) 2014 Taylor & Francis Group, London, ISBN 978-1-138-00124-4. Pages 943-947.

Otter, A., Murphy, J., Pakrashi, V., Robertson, A., Desmond, C. (2021). A review of modelling techniques for floating offshore wind turbines. Wind Energy. https://doi.org/10.1002/we.2701

Paine, R., Beards, C., Tucker, P., Bacon, D. H. (1994). Mechanical engineering principles. In E. H. Smith (Ed.), Mechanical Engineer's Reference Book (Twelfth Edition, pp. 1-1-1–48). Butterworth-Heinemann.

Penalba, M., Kelly, T., Ringwood, J. v., (2017). Using NEMOH for Modelling Wave Energy Converters: A Comparative Study with WAMIT. In: 12th European Wave and Tidal Energy Conference. Cork, Ireland.

Ren, Y., Venugopal, V., Shi, W. (2022). Dynamic analysis of a multi-column TLP floating offshore wind turbine with tendon failure scenarios. Ocean Engineering, 245, 110472.

Rezaei, R., Ghofranfarid, M.. (2018). Rural households' renewable energy usage intention in Iran: Extending the unified theory of acceptance and use of technology. Renew. Energy. 122, 382–391.

Riahi, K., Dentener, F., Gielen, D., Grubler, A., Jewell, J., Klimont, Z., Krey, D. McCollum, Pachauri, S., Rao, S., B. van Ruijven, D. van Vuuren, Wilson, C., (2012). Global Energy Assessment Chapter 17: Energy Pathways for Sustainable Development, Cambridge University press.

Robertson, A.N. , Jonkman, J.M.. (2011). Loads analysis of several offshore floating wind turbine concepts. In: 21st International Offshore and Polar Engineering conference, no. NREL/CP-5000-50539.

Sharma, N. and Dean. R., "Second-order directional seas and associated wave forces," Society of Petroleum Engineers Journal, 4:129-140, 1981.

United Nations Department of Economic and Social Affairs (UN DESA), (2017). Sustainable Development Goal 7: Ensure Access to Affordable, Reliable, Sustainable and Modern Energy for All, UN DESA, New York, USA.

Uzunoglu, E., Soares, C. G., (2019). A system for the hydrodynamic design of tension leg platforms of floating wind turbines. Ocean Engineering, 171, 78–92.

Uzunoglu, E., Soares, C. G., (2020). Hydrodynamic design of a free-float capable tension leg platform for a 10 MW wind turbine. Ocean Engineering, 197.

Uzunoglu, E., Oguz, E., Soares, C. G. (2021). An Overview of Platform Types Used in Floating Wind Energy. In: 2nd International Congress on Ship and Marine Technology (GMO-SHIPMAR 2021), Istanbul, Turkey.

WAMIT Inc., (2013). WAMIT v7.0 manual.

Wehmeyer, C., Ferri, F., Andersen, M. T., & Pedersen, R. R. (2014). Hybrid Model Representation of a TLP Including Flexible Topsides in Nonlinear Regular Waves. Energies, 7(8), 5047–5064.

van Vliet, B. (2012), Renewable Resources. In: Southerton, D. Encyclopedia of Consumer Culture. Thousand Oaks, California, USA. SAGE Publications, p1212-1214.

Yingyi, L. (2019). HAMS: A Frequency-Domain Preprocessor for Wave-Structure Interactions—Theory, Development, and Application. Journal of Marine Science and Engineering, 7: 81.

Zhao, Z., Shi, W., Wang, W., Qi, S., Li, X., (2021). Dynamic analysis of a novel semi-submersible platform for a 10 MW wind turbine in intermediate water depth. Ocean Eng. 237, 109688.

APPENDICES

A. FAST Input Files for Free Decay Test of Surge Motion

FDT for 3000 Sec in Surge Mod	
Parameter	*Value*
*.fst	
CompInflow	0
CompAero	0
Tmax	3000
DT	0.01
DT_out	0.01
*_HydroDyn.dat	
WaveDirMod	0
*ElastoDyn.dat	
PtfmSurge	1
*_FEAMooring.dat	
MaxIter	250000

```
------- FAST v8.16.* INPUT FILE -------------------------------------------------
---------------------- SIMULATION CONTROL --------------------------------------
False         Echo            - Echo input data to <RootName>.ech (flag)
"FATAL"       AbortLevel      - Error level when simulation should abort (string) {"WARNING", "SEVERE", "FATAL"}
       3000   TMax            - Total run time (s)
       0.01   DT              - Recommended module time step (s)
          2   InterpOrder     - Interpolation order for input/output time history (-) {1=linear, 2=quadratic}
          0   NumCrctn        - Number of correction iterations (-) {0=explicit calculation, i.e., no corrections}
      99999   DT_UJac         - Time between calls to get Jacobians (s)
     1E+06    UJacSclFact     - Scaling factor used in Jacobians (-)
---------------------- FEATURE SWITCHES AND FLAGS ------------------------------
          1   CompElast       - Compute structural dynamics (switch) {1=ElastoDyn; 2=ElastoDyn + BeamDyn for blades}
          0   CompInflow      - Compute inflow wind velocities (switch) {0=still air; 1=InflowWind; 2=external from OpenFOAM}
          0   CompAero        - Compute aerodynamic loads (switch) {0=None; 1=AeroDyn v14; 2=AeroDyn v15}
          1   CompServo       - Compute control and electrical-drive dynamics (switch) {0=None; 1=ServoDyn}
          1   CompHydro       - Compute hydrodynamic loads (switch) {0=None; 1=HydroDyn}
          0   CompSub         - Compute sub-structural dynamics (switch) {0=None; 1=SubDyn}
          2   CompMooring     - Compute mooring system (switch) {0=None; 1=MAP++; 2=FEAMooring; 3=MoorDyn; 4=OrcaFlex}
          0   CompIce         - Compute ice loads (switch) {0=None; 1=IceFloe; 2=IceDyn}
---------------------- INPUT FILES ---------------------------------------------
"NRELOffshrBsline5MW_MIT_NREL_TLP_ElastoDyn.dat"    EDFile          - Name of file containing ElastoDyn input parameters (quoted string)
"NRELOffshrBsline5MW_BeamDyn.dat"    BDBldFile(1)     - Name of file containing BeamDyn input parameters for blade 1 (quoted string)
"NRELOffshrBsline5MW_BeamDyn.dat"    BDBldFile(2)     - Name of file containing BeamDyn input parameters for blade 2 (quoted string)
"NRELOffshrBsline5MW_BeamDyn.dat"    BDBldFile(3)     - Name of file containing BeamDyn input parameters for blade 3 (quoted string)
"NRELOffshrBsline5MW_InflowWind.dat"    InflowFile      - Name of file containing inflow wind input parameters (quoted string)
"NRELOffshrBsline5MW_Onshore_AeroDyn15.dat"    AeroFile        - Name of file containing aerodynamic input parameters (quoted string)
"NRELOffshrBsline5MW_MIT_NREL_TLP_ServoDyn.dat"    ServoFile       - Name of file containing control and electrical-drive input parameters (quoted string)
"NRELOffshrBsline5MW_MIT_NREL_TLP_HydroDyn.dat"    HydroFile       - Name of file containing hydrodynamic input parameters (quoted string)
"unused"      SubFile         - Name of file containing sub-structural input parameters (quoted string)
"NRELOffshrBsline5MW_MIT_NREL_TLP_FEAMooring.dat"    MooringFile     - Name of file containing mooring system input parameters (quoted string)
"unused"      IceFile         - Name of file containing ice input parameters (quoted string)
---------------------- OUTPUT --------------------------------------------------
True          SumPrint        - Print summary data to "<RootName>.sum" (flag)
          1   SttsTime        - Amount of time between screen status messages (s)
       1000   ChkptTime       - Amount of time between creating checkpoint files for potential restart (s)
       0.01   DT_Out          - Time step for tabular output (s) (or "default")
          0   TStart          - Time to begin tabular output (s)
          1   OutFileFmt      - Format for tabular (time-marching) output file (switch) {1: text file [<RootName>.out], 2: binary file [<RootName>.outb], 3: both}
True          TabDelim        - Use tab delimiters in text tabular output file? (flag) {uses spaces if false}
"ES10.3E2"    OutFmt          - Format used for text tabular output, excluding the time channel.  Resulting field should be 10 characters. (quoted string)
```

```
---------------------- FAST MOORING FILE -----------------------------------------
---------------------- SIMULATION CONTROL ----------------------------------------
False             Echo         - Echo input data to <RootName>.ech (flag)
  default         DT           - Communication interval for module (s)
      6           NumLines     - Number of lines
     20           NumElem      - Total number of elements per line
  default         Gravity      - Gravitational acceleration (m/s^2)
  default         WtrDens      - Water density (kg/m^3)
    250000           MaxIter      - Maximum number of static iterations
    1e-4          Eps          - Static iteration tolerance


------- HydroDyn v2.03.* Input File ------------------------------------------
False             Echo           - Echo the input file data (flag)
---------------------- ENVIRONMENTAL CONDITIONS -------------------------------
          1025    WtrDens        - Water density (kg/m^3)
           150    WtrDpth        - Water depth (meters)
             0    MSL2SWL        - Offset between still-water level and mean sea level (meters) [positive upwar
---------------------- WAVES --------------------------------------------------
             0    WaveMod        - Incident wave kinematics model {0: none=still water, 1: regular (periodic),
             0    WaveStMod      - Model for stretching incident wave kinematics to instantaneous free surface
          3630    WaveTMax       - Analysis time for incident wave calculations (sec) [unused when WaveMod=0; d
          0.25    WaveDT         - Time step for incident wave calculations     (sec) [unused when WaveMod=0; 0
          12.7    WaveHs         - Significant wave height of incident waves (meters) [used only when WaveMod=1
          14.1    WaveTp         - Peak-spectral period of incident waves       (sec) [used only when WaveMod=1
"DEFAULT"         WavePkShp      - Peak-shape parameter of incident wave spectrum (-) or DEFAULT (string) [used
             0    WvLowCOff      - Low  cut-off frequency or lower frequency limit of the wave spectrum beyond
           500    WvHiCOff       - High cut-off frequency or upper frequency limit of the wave spectrum beyond
           180     WaveDir        - Incident wave propagation heading direction                          (degree
             0    WaveDirMod     - Directional spreading function {0: none, 1: COS2S}                  (-)
             1    WaveDirSpread  - Wave direction spreading coefficient ( > 0 )                        (-)
             1     WaveNDir       - Number of wave directions                                           (-)
            10    WaveDirRange   - Range of wave directions (full range: WaveDir +/- 1/2*WaveDirRange) (degrees
     123456789    WaveSeed(1)    - First  random seed of incident waves [-2147483648 to 2147483647]    (-)
    1011121314    WaveSeed(2)    - Second random seed of incident waves [-2147483648 to 2147483647]    (-)
TRUE              WaveNDAmp      - Flag for normally distributed amplitudes                            (flag)
""                WvKinFile      - Root name of externally generated wave data file(s)        (quoted string)
             1    NWaveElev      - Number of points where the incident wave elevations can be computed (-)
             0    WaveElevxi     - List of xi-coordinates for points where the incident wave elevations can be
             0    WaveElevyi     - List of yi-coordinates for points where the incident wave elevations can be
```

```
------- ELASTODYN v1.03.* INPUT FILE -------------------------------------------
---------------------- SIMULATION CONTROL --------------------------------------
False          Echo        - Echo input data to "<RootName>.ech" (flag)
          3    Method      - Integration method: {1: RK4, 2: AB4, or 3: ABM4} (-)
"default"      DT          - Integration time step (s)
---------------------- ENVIRONMENTAL CONDITION ---------------------------------
    9.80665    Gravity     - Gravitational acceleration (m/s^2)
---------------------- DEGREES OF FREEDOM --------------------------------------
True           FlapDOF1    - First flapwise blade mode DOF (flag)
True           FlapDOF2    - Second flapwise blade mode DOF (flag)
True           EdgeDOF     - First edgewise blade mode DOF (flag)
False          TeetDOF     - Rotor-teeter DOF (flag) [unused for 3 blades]
True           DrTrDOF     - Drivetrain rotational-flexibility DOF (flag)
True           GenDOF      - Generator DOF (flag)
True           YawDOF      - Yaw DOF (flag)
True           TwFADOF1    - First fore-aft tower bending-mode DOF (flag)
True           TwFADOF2    - Second fore-aft tower bending-mode DOF (flag)
True           TwSSDOF1    - First side-to-side tower bending-mode DOF (flag)
True           TwSSDOF2    - Second side-to-side tower bending-mode DOF (flag)
True           PtfmSgDOF   - Platform horizontal surge translation DOF (flag)
True           PtfmSwDOF   - Platform horizontal sway translation DOF (flag)
True           PtfmHvDOF   - Platform vertical heave translation DOF (flag)
True           PtfmRDOF    - Platform roll tilt rotation DOF (flag)
True           PtfmPDOF    - Platform pitch tilt rotation DOF (flag)
True           PtfmYDOF    - Platform yaw rotation DOF (flag)
---------------------- INITIAL CONDITIONS --------------------------------------
           0   OoPDefl     - Initial out-of-plane blade-tip displacement (meters)
           0   IPDefl      - Initial in-plane blade-tip deflection (meters)
           0   BlPitch(1)  - Blade 1 initial pitch (degrees)
           0   BlPitch(2)  - Blade 2 initial pitch (degrees)
           0   BlPitch(3)  - Blade 3 initial pitch (degrees) [unused for 2 blades]
           0   TeetDefl    - Initial or fixed teeter angle (degrees) [unused for 3 blades]
           0   Azimuth     - Initial azimuth angle for blade 1 (degrees)
        12.1   RotSpeed    - Initial or fixed rotor speed (rpm)
           0   NacYaw      - Initial or fixed nacelle-yaw angle (degrees)
           0   TTDspFA     - Initial fore-aft tower-top displacement (meters)
           0   TTDspSS     - Initial side-to-side tower-top displacement (meters)
           1   PtfmSurge   - Initial or fixed horizontal surge translational displacement of platform (meters)
           0   PtfmSway    - Initial or fixed horizontal sway translational displacement of platform (meters)
           0   PtfmHeave   - Initial or fixed vertical heave translational displacement of platform (meters)
           0   PtfmRoll    - Initial or fixed roll tilt rotational displacement of platform (degrees)
           0   PtfmPitch   - Initial or fixed pitch tilt rotational displacement of platform (degrees)
           0   PtfmYaw     - Initial or fixed yaw rotational displacement of platform (degrees)
```

B. FAST Input Files for Free Decay Test of Surge Motion

FDT for 100 Sec in Surge Mod	
Parameter	*Value*
*.fst	
CompInflow	0
CompAero	0
Tmax	3000
DT	0.01
DT_out	0.01
*_HydroDyn.dat	
WaveDirMod	0
*ElastoDyn.dat	
PtfmSurge	1
*_FEAMooring.dat	
MaxIter	250000

```
------- FAST v8.16.* INPUT FILE -------------------------------------------------
---------------------- SIMULATION CONTROL --------------------------------------
False         Echo            - Echo input data to <RootName>.ech (flag)
"FATAL"       AbortLevel      - Error level when simulation should abort (string) {"WARNING", "SEVERE", "FATAL"}
      100   TMax            - Total run time (s)
     0.01   DT              - Recommended module time step (s)
        2   InterpOrder     - Interpolation order for input/output time history (-) {1=linear, 2=quadratic}
        0   NumCrctn        - Number of correction iterations (-) {0=explicit calculation, i.e., no corrections}
    99999   DT_UJac         - Time between calls to get Jacobians (s)
    1E+06   UJacSclFact     - Scaling factor used in Jacobians (-)
---------------------- FEATURE SWITCHES AND FLAGS ------------------------------
        1   CompElast       - Compute structural dynamics (switch) {1=ElastoDyn; 2=ElastoDyn + BeamDyn for blades}
        0   CompInflow      - Compute inflow wind velocities (switch) {0=still air; 1=InflowWind; 2=external from OpenFOAM}
        0   CompAero        - Compute aerodynamic loads (switch) {0=None; 1=AeroDyn v14; 2=AeroDyn v15}
        1   CompServo       - Compute control and electrical-drive dynamics (switch) {0=None; 1=ServoDyn}
        1   CompHydro       - Compute hydrodynamic loads (switch) {0=None; 1=HydroDyn}
        0   CompSub         - Compute sub-structural dynamics (switch) {0=None; 1=SubDyn}
        2   CompMooring     - Compute mooring system (switch) {0=None; 1=MAP++; 2=FEAMooring; 3=MoorDyn; 4=OrcaFlex}
        0   CompIce         - Compute ice loads (switch) {0=None; 1=IceFloe; 2=IceDyn}
---------------------- INPUT FILES ---------------------------------------------
"NRELOffshrBslineSMW_MIT_NREL_TLP_ElastoDyn.dat"    EDFile          - Name of file containing ElastoDyn input parameters (quoted string)
"NRELOffshrBslineSMW_BeamDyn.dat"    BDBldFile(1)    - Name of file containing BeamDyn input parameters for blade 1 (quoted string)
"NRELOffshrBslineSMW_BeamDyn.dat"    BDBldFile(2)    - Name of file containing BeamDyn input parameters for blade 2 (quoted string)
"NRELOffshrBslineSMW_BeamDyn.dat"    BDBldFile(3)    - Name of file containing BeamDyn input parameters for blade 3 (quoted string)
"NRELOffshrBslineSMW_InflowWind.dat"    InflowFile      - Name of file containing inflow wind input parameters (quoted string)
"NRELOffshrBslineSMW_Onshore_AeroDyn15.dat"    AeroFile        - Name of file containing aerodynamic input parameters (quoted string)
"NRELOffshrBslineSMW_MIT_NREL_TLP_ServoDyn.dat"    ServoFile       - Name of file containing control and electrical-drive input parameters (quoted string)
"NRELOffshrBslineSMW_MIT_NREL_TLP_HydroDyn.dat"    HydroFile       - Name of file containing hydrodynamic input parameters (quoted string)
"unused"      SubFile         - Name of file containing sub-structural input parameters (quoted string)
"NRELOffshrBslineSMW_MIT_NREL_TLP_FEAMooring.dat"    MooringFile     - Name of file containing mooring system input parameters (quoted string)
"unused"      IceFile         - Name of file containing ice input parameters (quoted string)
---------------------- OUTPUT --------------------------------------------------
True          SumPrint        - Print summary data to "<RootName>.sum" (flag)
        1   SttsTime        - Amount of time between screen status messages (s)
     1000   ChkptTime       - Amount of time between creating checkpoint files for potential restart (s)
     0.01   DT_Out          - Time step for tabular output (s) (or "default")
        0   TStart          - Time to begin tabular output (s)
        1   OutFileFmt      - Format for tabular (time-marching) output file (switch) {1: text file [<RootName>.out], 2: binary file [<RootName>.outb], 3: both}
True          TabDelim        - Use tab delimiters in text tabular output file? (flag) {uses spaces if false}
"ES10.3E2"    OutFmt          - Format used for text tabular output, excluding the time channel.  Resulting field should be 10 characters. (quoted string)
                    -------------
```

```
---------------------- FAST MOORING FILE -----------------------------------
---------------------- SIMULATION CONTROL ----------------------------------
False             Echo          - Echo input data to <RootName>.ech (flag)
  default         DT            - Communication interval for module (s)
        6         NumLines      - Number of lines
       20         NumElem       - Total number of elements per line
  default         Gravity       - Gravitational acceleration (m/s^2)
  default         WtrDens       - Water density (kg/m^3)
    250000           MaxIter       - Maximum number of static iterations
    1e-4          Eps           - Static iteration tolerance
```

```
------- HydroDyn v2.03.* Input File ------------------------------------------
False             Echo          - Echo the input file data (flag)
---------------------- ENVIRONMENTAL CONDITIONS --------------------------------
          1025    WtrDens       - Water density (kg/m^3)
           150    WtrDpth       - Water depth (meters)
             0    MSL2SWL       - Offset between still-water level and mean sea level (meters) [positive upwar
---------------------- WAVES ---------------------------------------------------
             0    WaveMod       - Incident wave kinematics model {0: none=still water, 1: regular (periodic),
             0    WaveStMod     - Model for stretching incident wave kinematics to instantaneous free surface
          3630    WaveTMax      - Analysis time for incident wave calculations (sec) [unused when WaveMod=0; d
          0.25    WaveDT        - Time step for incident wave calculations     (sec) [unused when WaveMod=0; 0
          12.7    WaveHs        - Significant wave height of incident waves (meters) [used only when WaveMod=1
          14.1    WaveTp        - Peak-spectral period of incident waves       (sec) [used only when WaveMod=1
"DEFAULT"         WavePkShp     - Peak-shape parameter of incident wave spectrum (-) or DEFAULT (string) [used
             0    WvLowCOff     - Low  cut-off frequency or lower frequency limit of the wave spectrum beyond
           500    WvHiCOff      - High cut-off frequency or upper frequency limit of the wave spectrum beyond
           180     WaveDir       - Incident wave propagation heading direction                          (degree
             0    WaveDirMod    - Directional spreading function {0: none, 1: COS2S}                   (-)
             1    WaveDirSpread - Wave direction spreading coefficient ( > 0 )                         (-)
             1     WaveNDir      - Number of wave directions                                           (-)
            10    WaveDirRange  - Range of wave directions (full range: WaveDir +/- 1/2*WaveDirRange) (degrees
     123456789    WaveSeed(1)   - First  random seed of incident waves [-2147483648 to 2147483647]    (-)
    1011121314    WaveSeed(2)   - Second random seed of incident waves [-2147483648 to 2147483647]    (-)
TRUE              WaveNDAmp     - Flag for normally distributed amplitudes                             (flag)
""                WvKinFile     - Root name of externally generated wave data file(s)        (quoted string)
             1    NWaveElev     - Number of points where the incident wave elevations can be computed (-)
             0    WaveElevxi    - List of xi-coordinates for points where the incident wave elevations can be
             0    WaveElevyi    - List of yi-coordinates for points where the incident wave elevations can be
```

```
------- ELASTODYN v1.03.* INPUT FILE ------------------------------------------
---------------------- SIMULATION CONTROL --------------------------------------
False          Echo        - Echo input data to "<RootName>.ech" (flag)
           3   Method      - Integration method: {1: RK4, 2: AB4, or 3: ABM4} (-)
"default"      DT          - Integration time step (s)
---------------------- ENVIRONMENTAL CONDITION ---------------------------------
    9.80665    Gravity     - Gravitational acceleration (m/s^2)
---------------------- DEGREES OF FREEDOM --------------------------------------
True           FlapDOF1    - First flapwise blade mode DOF (flag)
True           FlapDOF2    - Second flapwise blade mode DOF (flag)
True           EdgeDOF     - First edgewise blade mode DOF (flag)
False          TeetDOF     - Rotor-teeter DOF (flag) [unused for 3 blades]
True           DrTrDOF     - Drivetrain rotational-flexibility DOF (flag)
True           GenDOF      - Generator DOF (flag)
True           YawDOF      - Yaw DOF (flag)
True           TwFADOF1    - First fore-aft tower bending-mode DOF (flag)
True           TwFADOF2    - Second fore-aft tower bending-mode DOF (flag)
True           TwSSDOF1    - First side-to-side tower bending-mode DOF (flag)
True           TwSSDOF2    - Second side-to-side tower bending-mode DOF (flag)
True           PtfmSgDOF   - Platform horizontal surge translation DOF (flag)
True           PtfmSwDOF   - Platform horizontal sway translation DOF (flag)
True           PtfmHvDOF   - Platform vertical heave translation DOF (flag)
True           PtfmRDOF    - Platform roll tilt rotation DOF (flag)
True           PtfmPDOF    - Platform pitch tilt rotation DOF (flag)
True           PtfmYDOF    - Platform yaw rotation DOF (flag)
---------------------- INITIAL CONDITIONS --------------------------------------
           0   OoPDefl     - Initial out-of-plane blade-tip displacement (meters)
           0   IPDefl      - Initial in-plane blade-tip deflection (meters)
           0   BlPitch(1)  - Blade 1 initial pitch (degrees)
           0   BlPitch(2)  - Blade 2 initial pitch (degrees)
           0   BlPitch(3)  - Blade 3 initial pitch (degrees) [unused for 2 blades]
           0   TeetDefl    - Initial or fixed teeter angle (degrees) [unused for 3 blades]
           0   Azimuth     - Initial azimuth angle for blade 1 (degrees)
        12.1   RotSpeed    - Initial or fixed rotor speed (rpm)
           0   NacYaw      - Initial or fixed nacelle-yaw angle (degrees)
           0   TTDspFA     - Initial fore-aft tower-top displacement (meters)
           0   TTDspSS     - Initial side-to-side tower-top displacement (meters)
           1   PtfmSurge   - Initial or fixed horizontal surge translational displacement of platform (meters)
           0   PtfmSway    - Initial or fixed horizontal sway translational displacement of platform (meters)
           0   PtfmHeave   - Initial or fixed vertical heave translational displacement of platform (meters)
           0   PtfmRoll    - Initial or fixed roll tilt rotational displacement of platform (degrees)
           0   PtfmPitch   - Initial or fixed pitch tilt rotational displacement of platform (degrees)
           0   PtfmYaw     - Initial or fixed yaw rotational displacement of platform (degrees)
```

C. FAST Input Files for Free Decay Test of Pitch Motion

FDT for 3000 Sec in Pitch Mod	
Parameter	*Value*
*.fst	
CompInflow	0
CompAero	0
Tmax	3000
DT	0.01
DT_out	0.01
*_HydroDyn.dat	
WaveDirMod	0
*ElastoDyn.dat	
PtfmPitch	0.1
*_FEAMooring.dat	
MaxIter	250000

```
------- FAST v8.16.* INPUT FILE -------------------------------------------------
---------------------- SIMULATION CONTROL --------------------------------------
False         Echo            - Echo input data to <RootName>.ech (flag)
"FATAL"       AbortLevel      - Error level when simulation should abort (string) {"WARNING", "SEVERE", "FATAL"}
      3000    TMax            - Total run time (s)
      0.01    DT              - Recommended module time step (s)
         2    InterpOrder     - Interpolation order for input/output time history (-) {1=linear, 2=quadratic}
         0    NumCrctn        - Number of correction iterations (-) {0=explicit calculation, i.e., no corrections}
     99999    DT_UJac         - Time between calls to get Jacobians (s)
     1E+06    UJacSclFact     - Scaling factor used in Jacobians (-)
---------------------- FEATURE SWITCHES AND FLAGS ------------------------------
         1    CompElast       - Compute structural dynamics (switch) {1=ElastoDyn; 2=ElastoDyn + BeamDyn for blades}
         0    CompInflow      - Compute inflow wind velocities (switch) {0=still air; 1=InflowWind; 2=external from OpenFOAM}
         0    CompAero        - Compute aerodynamic loads (switch) {0=None; 1=AeroDyn v14; 2=AeroDyn v15}
         1    CompServo       - Compute control and electrical-drive dynamics (switch) {0=None; 1=ServoDyn}
         1    CompHydro       - Compute hydrodynamic loads (switch) {0=None; 1=HydroDyn}
         0    CompSub         - Compute sub-structural dynamics (switch) {0=None; 1=SubDyn}
         2    CompMooring     - Compute mooring system (switch) {0=None; 1=MAP++; 2=FEAMooring; 3=MoorDyn; 4=OrcaFlex}
         0    CompIce         - Compute ice loads (switch) {0=None; 1=IceFloe; 2=IceDyn}
---------------------- INPUT FILES ---------------------------------------------
"NRELOffshrBsline5MW_MIT_NREL_TLP_ElastoDyn.dat"    EDFile          - Name of file containing ElastoDyn input parameters (quoted string)
"NRELOffshrBsline5MW_BeamDyn.dat"    BDBldFile(1)    - Name of file containing BeamDyn input parameters for blade 1 (quoted string)
"NRELOffshrBsline5MW_BeamDyn.dat"    BDBldFile(2)    - Name of file containing BeamDyn input parameters for blade 2 (quoted string)
"NRELOffshrBsline5MW_BeamDyn.dat"    BDBldFile(3)    - Name of file containing BeamDyn input parameters for blade 3 (quoted string)
"NRELOffshrBsline5MW_InflowWind.dat"    InflowFile      - Name of file containing inflow wind input parameters (quoted string)
"NRELOffshrBsline5MW_Onshore_AeroDyn15.dat"    AeroFile        - Name of file containing aerodynamic input parameters (quoted string)
"NRELOffshrBsline5MW_MIT_NREL_TLP_ServoDyn.dat"    ServoFile       - Name of file containing control and electrical-drive input parameters (quoted string)
"NRELOffshrBsline5MW_MIT_NREL_TLP_HydroDyn.dat"    HydroFile       - Name of file containing hydrodynamic input parameters (quoted string)
"unused"      SubFile         - Name of file containing sub-structural input parameters (quoted string)
"NRELOffshrBsline5MW_MIT_NREL_TLP_FEAMooring.dat"    MooringFile     - Name of file containing mooring system input parameters (quoted string)
"unused"      IceFile         - Name of file containing ice input parameters (quoted string)
---------------------- OUTPUT --------------------------------------------------
True          SumPrint        - Print summary data to "<RootName>.sum" (flag)
         1    SttsTime        - Amount of time between screen status messages (s)
      1000    ChkptTime       - Amount of time between creating checkpoint files for potential restart (s)
      0.01    DT_Out          - Time step for tabular output (s) (or "default")
         0    TStart          - Time to begin tabular output (s)
         1    OutFileFmt      - Format for tabular (time-marching) output file (switch) {1: text file [<RootName>.out], 2: binary file [<RootName>.outb], 3: both}
True          TabDelim        - Use tab delimiters in text tabular output file? (flag) {uses spaces if false}
"ES10.3E2"    OutFmt          - Format used for text tabular output, excluding the time channel.  Resulting field should be 10 characters. (quoted string)
```

```
---------------------- FAST MOORING FILE -----------------------------------
---------------------- SIMULATION CONTROL ----------------------------------
False             Echo          - Echo input data to <RootName>.ech (flag)
  default         DT            - Communication interval for module (s)
        6         NumLines      - Number of lines
       20         NumElem       - Total number of elements per line
  default         Gravity       - Gravitational acceleration (m/s^2)
  default         WtrDens       - Water density (kg/m^3)
    250000           MaxIter      - Maximum number of static iterations
    1e-4          Eps           - Static iteration tolerance
```

```
------- HydroDyn v2.03.* Input File ------------------------------------------
False             Echo          - Echo the input file data (flag)
---------------------- ENVIRONMENTAL CONDITIONS --------------------------------
          1025    WtrDens       - Water density (kg/m^3)
           150    WtrDpth       - Water depth (meters)
             0    MSL2SWL       - Offset between still-water level and mean sea level (meters) [positive upwar
---------------------- WAVES ---------------------------------------------------
             0    WaveMod       - Incident wave kinematics model {0: none=still water, 1: regular (periodic),
             0    WaveStMod     - Model for stretching incident wave kinematics to instantaneous free surface
          3630    WaveTMax      - Analysis time for incident wave calculations (sec) [unused when WaveMod=0; d
          0.25    WaveDT        - Time step for incident wave calculations     (sec) [unused when WaveMod=0; 0
          12.7    WaveHs        - Significant wave height of incident waves (meters) [used only when WaveMod=1
          14.1    WaveTp        - Peak-spectral period of incident waves       (sec) [used only when WaveMod=1
"DEFAULT"         WavePkShp     - Peak-shape parameter of incident wave spectrum (-) or DEFAULT (string) [used
             0    WvLowCOff     - Low  cut-off frequency or lower frequency limit of the wave spectrum beyond
           500    WvHiCOff      - High cut-off frequency or upper frequency limit of the wave spectrum beyond
           180     WaveDir       - Incident wave propagation heading direction                          (degree
             0    WaveDirMod    - Directional spreading function {0: none, 1: COS2S}                  (-)
             1    WaveDirSpread - Wave direction spreading coefficient ( > 0 )                        (-)
             1     WaveNDir      - Number of wave directions                                           (-)
            10    WaveDirRange  - Range of wave directions (full range: WaveDir +/- 1/2*WaveDirRange) (degrees
     123456789    WaveSeed(1)   - First  random seed of incident waves [-2147483648 to 2147483647]    (-)
    1011121314    WaveSeed(2)   - Second random seed of incident waves [-2147483648 to 2147483647]    (-)
TRUE              WaveNDAmp     - Flag for normally distributed amplitudes                            (flag)
""                WvKinFile     - Root name of externally generated wave data file(s)        (quoted string)
             1    NWaveElev     - Number of points where the incident wave elevations can be computed (-)
             0    WaveElevxi    - List of xi-coordinates for points where the incident wave elevations can be
             0    WaveElevyi    - List of yi-coordinates for points where the incident wave elevations can be
```

```
------- ELASTODYN v1.03.* INPUT FILE ------------------------------------------
---------------------- SIMULATION CONTROL --------------------------------------
False          Echo        - Echo input data to "<RootName>.ech" (flag)
          3    Method      - Integration method: {1: RK4, 2: AB4, or 3: ABM4} (-)
"default"      DT          - Integration time step (s)
---------------------- ENVIRONMENTAL CONDITION ---------------------------------
    9.80665    Gravity     - Gravitational acceleration (m/s^2)
---------------------- DEGREES OF FREEDOM --------------------------------------
True           FlapDOF1    - First flapwise blade mode DOF (flag)
True           FlapDOF2    - Second flapwise blade mode DOF (flag)
True           EdgeDOF     - First edgewise blade mode DOF (flag)
False          TeetDOF     - Rotor-teeter DOF (flag) [unused for 3 blades]
True           DrTrDOF     - Drivetrain rotational-flexibility DOF (flag)
True           GenDOF      - Generator DOF (flag)
True           YawDOF      - Yaw DOF (flag)
True           TwFADOF1    - First fore-aft tower bending-mode DOF (flag)
True           TwFADOF2    - Second fore-aft tower bending-mode DOF (flag)
True           TwSSDOF1    - First side-to-side tower bending-mode DOF (flag)
True           TwSSDOF2    - Second side-to-side tower bending-mode DOF (flag)
True           PtfmSgDOF   - Platform horizontal surge translation DOF (flag)
True           PtfmSwDOF   - Platform horizontal sway translation DOF (flag)
True           PtfmHvDOF   - Platform vertical heave translation DOF (flag)
True           PtfmRDOF    - Platform roll tilt rotation DOF (flag)
True           PtfmPDOF    - Platform pitch tilt rotation DOF (flag)
True           PtfmYDOF    - Platform yaw rotation DOF (flag)
---------------------- INITIAL CONDITIONS --------------------------------------
          0    OoPDefl     - Initial out-of-plane blade-tip displacement (meters)
          0    IPDefl      - Initial in-plane blade-tip deflection (meters)
          0    BlPitch(1)  - Blade 1 initial pitch (degrees)
          0    BlPitch(2)  - Blade 2 initial pitch (degrees)
          0    BlPitch(3)  - Blade 3 initial pitch (degrees) [unused for 2 blades]
          0    TeetDefl    - Initial or fixed teeter angle (degrees) [unused for 3 blades]
          0    Azimuth     - Initial azimuth angle for blade 1 (degrees)
       12.1    RotSpeed    - Initial or fixed rotor speed (rpm)
          0    NacYaw      - Initial or fixed nacelle-yaw angle (degrees)
          0    TTDspFA     - Initial fore-aft tower-top displacement (meters)
          0    TTDspSS     - Initial side-to-side tower-top displacement (meters)
          0    PtfmSurge   - Initial or fixed horizontal surge translational displacement of platform (meters)
          0    PtfmSway    - Initial or fixed horizontal sway translational displacement of platform (meters)
          0    PtfmHeave   - Initial or fixed vertical heave translational displacement of platform (meters)
          0    PtfmRoll    - Initial or fixed roll tilt rotational displacement of platform (degrees)
        0.1    PtfmPitch   - Initial or fixed pitch tilt rotational displacement of platform (degrees)
          0    PtfmYaw     - Initial or fixed yaw rotational displacement of platform (degrees)
```

D. FAST Input Files for Free Decay Test of Pitch Motion

FDT for 100 Sec in Pitch Mod

Parameter	*Value*
*.fst	
CompInflow	0
CompAero	0
Tmax	3000
DT	0.01
DT_out	0.01
*_HydroDyn.dat	
WaveDirMod	0
*ElastoDyn.dat	
PtfmPitch	0.1
*_FEAMooring.dat	
MaxIter	250000

```
------- FAST v8.16.* INPUT FILE -------------------------------------------------
---------------------- SIMULATION CONTROL --------------------------------------
False         Echo            - Echo input data to <RootName>.ech (flag)
"FATAL"       AbortLevel      - Error level when simulation should abort (string) {"WARNING", "SEVERE", "FATAL"}
      100   TMax            - Total run time (s)
     0.01   DT              - Recommended module time step (s)
        2   InterpOrder     - Interpolation order for input/output time history (-) {1=linear, 2=quadratic}
        0   NumCrctn        - Number of correction iterations (-) {0=explicit calculation, i.e., no corrections}
    99999   DT_UJac         - Time between calls to get Jacobians (s)
    1E+06   UJacSclFact     - Scaling factor used in Jacobians (-)
---------------------- FEATURE SWITCHES AND FLAGS ------------------------------
        1   CompElast       - Compute structural dynamics (switch) {1=ElastoDyn; 2=ElastoDyn + BeamDyn for blades}
        0   CompInflow      - Compute inflow wind velocities (switch) {0=still air; 1=InflowWind; 2=external from OpenFOAM}
        0   CompAero        - Compute aerodynamic loads (switch) {0=None; 1=AeroDyn v14; 2=AeroDyn v15}
        1   CompServo       - Compute control and electrical-drive dynamics (switch) {0=None; 1=ServoDyn}
        1   CompHydro       - Compute hydrodynamic loads (switch) {0=None; 1=HydroDyn}
        0   CompSub         - Compute sub-structural dynamics (switch) {0=None; 1=SubDyn}
        2   CompMooring     - Compute mooring system (switch) {0=None; 1=MAP++; 2=FEAMooring; 3=MoorDyn; 4=OrcaFlex}
        0   CompIce         - Compute ice loads (switch) {0=None; 1=IceFloe; 2=IceDyn}
---------------------- INPUT FILES ---------------------------------------------
"NRELOffshrBslineSMW_MIT_NREL_TLP_ElastoDyn.dat"    EDFile          - Name of file containing ElastoDyn input parameters (quoted string)
"NRELOffshrBslineSMW_BeamDyn.dat"    BDBldFile(1)    - Name of file containing BeamDyn input parameters for blade 1 (quoted string)
"NRELOffshrBslineSMW_BeamDyn.dat"    BDBldFile(2)    - Name of file containing BeamDyn input parameters for blade 2 (quoted string)
"NRELOffshrBslineSMW_BeamDyn.dat"    BDBldFile(3)    - Name of file containing BeamDyn input parameters for blade 3 (quoted string)
"NRELOffshrBslineSMW_InflowWind.dat"    InflowFile      - Name of file containing inflow wind input parameters (quoted string)
"NRELOffshrBslineSMW_Onshore_AeroDyn15.dat"    AeroFile        - Name of file containing aerodynamic input parameters (quoted string)
"NRELOffshrBslineSMW_MIT_NREL_TLP_ServoDyn.dat"    ServoFile       - Name of file containing control and electrical-drive input parameters (quoted string)
"NRELOffshrBslineSMW_MIT_NREL_TLP_HydroDyn.dat"    HydroFile       - Name of file containing hydrodynamic input parameters (quoted string)
"unused"      SubFile         - Name of file containing sub-structural input parameters (quoted string)
"NRELOffshrBslineSMW_MIT_NREL_TLP_FEAMooring.dat"    MooringFile     - Name of file containing mooring system input parameters (quoted string)
"unused"      IceFile         - Name of file containing ice input parameters (quoted string)
---------------------- OUTPUT --------------------------------------------------
True          SumPrint        - Print summary data to "<RootName>.sum" (flag)
        1   SttsTime        - Amount of time between screen status messages (s)
     1000   ChkptTime       - Amount of time between creating checkpoint files for potential restart (s)
     0.01   DT_Out          - Time step for tabular output (s) (or "default")
        0   TStart          - Time to begin tabular output (s)
        1   OutFileFmt      - Format for tabular (time-marching) output file (switch) {1: text file [<RootName>.out], 2: binary file [<RootName>.outb], 3: both}
True          TabDelim        - Use tab delimiters in text tabular output file? (flag) {uses spaces if false}
"ES10.3E2"    OutFmt          - Format used for text tabular output, excluding the time channel.  Resulting field should be 10 characters. (quoted string)
                  ------------
```

```
---------------------- FAST MOORING FILE -----------------------------------
---------------------- SIMULATION CONTROL ----------------------------------
False             Echo          - Echo input data to <RootName>.ech (flag)
  default         DT            - Communication interval for module (s)
     6            NumLines      - Number of lines
    20            NumElem       - Total number of elements per line
  default         Gravity       - Gravitational acceleration (m/s^2)
  default         WtrDens       - Water density (kg/m^3)
    250000           MaxIter       - Maximum number of static iterations
    1e-4          Eps           - Static iteration tolerance
```

```
------- HydroDyn v2.03.* Input File ------------------------------------------
False            Echo          - Echo the input file data (flag)
---------------------- ENVIRONMENTAL CONDITIONS --------------------------------
          1025   WtrDens       - Water density (kg/m^3)
           150   WtrDpth       - Water depth (meters)
             0   MSL2SWL       - Offset between still-water level and mean sea level (meters) [positive upwar
---------------------- WAVES ---------------------------------------------------
             0   WaveMod       - Incident wave kinematics model {0: none=still water, 1: regular (periodic),
             0   WaveStMod     - Model for stretching incident wave kinematics to instantaneous free surface
          3630   WaveTMax      - Analysis time for incident wave calculations (sec) [unused when WaveMod=0; d
          0.25   WaveDT        - Time step for incident wave calculations     (sec) [unused when WaveMod=0; 0
          12.7   WaveHs        - Significant wave height of incident waves (meters) [used only when WaveMod=1
          14.1   WaveTp        - Peak-spectral period of incident waves       (sec) [used only when WaveMod=1
"DEFAULT"        WavePkShp     - Peak-shape parameter of incident wave spectrum (-) or DEFAULT (string) [used
             0   WvLowCOff     - Low  cut-off frequency or lower frequency limit of the wave spectrum beyond
           500   WvHiCOff      - High cut-off frequency or upper frequency limit of the wave spectrum beyond
           180    WaveDir       - Incident wave propagation heading direction                          (degree
             0   WaveDirMod    - Directional spreading function {0: none, 1: COS2S}                  (-)
             1   WaveDirSpread - Wave direction spreading coefficient ( > 0 )                        (-)
             1    WaveNDir      - Number of wave directions                                           (-)
            10   WaveDirRange  - Range of wave directions (full range: WaveDir +/- 1/2*WaveDirRange) (degrees
     123456789   WaveSeed(1)   - First  random seed of incident waves [-2147483648 to 2147483647]    (-)
    1011121314   WaveSeed(2)   - Second random seed of incident waves [-2147483648 to 2147483647]    (-)
TRUE             WaveNDAmp     - Flag for normally distributed amplitudes                           (flag)
""               WvKinFile     - Root name of externally generated wave data file(s)        (quoted string)
             1   NWaveElev     - Number of points where the incident wave elevations can be computed (-)
             0   WaveElevxi    - List of xi-coordinates for points where the incident wave elevations can be
             0   WaveElevyi    - List of yi-coordinates for points where the incident wave elevations can be
```

```
------- ELASTODYN v1.03.* INPUT FILE ------------------------------------------
---------------------- SIMULATION CONTROL --------------------------------------
False         Echo        - Echo input data to "<RootName>.ech" (flag)
          3   Method      - Integration method: {1: RK4, 2: AB4, or 3: ABM4} (-)
"default"     DT          - Integration time step (s)
---------------------- ENVIRONMENTAL CONDITION ---------------------------------
    9.80665   Gravity     - Gravitational acceleration (m/s^2)
---------------------- DEGREES OF FREEDOM --------------------------------------
True          FlapDOF1    - First flapwise blade mode DOF (flag)
True          FlapDOF2    - Second flapwise blade mode DOF (flag)
True          EdgeDOF     - First edgewise blade mode DOF (flag)
False         TeetDOF     - Rotor-teeter DOF (flag) [unused for 3 blades]
True          DrTrDOF     - Drivetrain rotational-flexibility DOF (flag)
True          GenDOF      - Generator DOF (flag)
True          YawDOF      - Yaw DOF (flag)
True          TwFADOF1    - First fore-aft tower bending-mode DOF (flag)
True          TwFADOF2    - Second fore-aft tower bending-mode DOF (flag)
True          TwSSDOF1    - First side-to-side tower bending-mode DOF (flag)
True          TwSSDOF2    - Second side-to-side tower bending-mode DOF (flag)
True          PtfmSgDOF   - Platform horizontal surge translation DOF (flag)
True          PtfmSwDOF   - Platform horizontal sway translation DOF (flag)
True          PtfmHvDOF   - Platform vertical heave translation DOF (flag)
True          PtfmRDOF    - Platform roll tilt rotation DOF (flag)
True          PtfmPDOF    - Platform pitch tilt rotation DOF (flag)
True          PtfmYDOF    - Platform yaw rotation DOF (flag)
---------------------- INITIAL CONDITIONS --------------------------------------
          0   OoPDefl     - Initial out-of-plane blade-tip displacement (meters)
          0   IPDefl      - Initial in-plane blade-tip deflection (meters)
          0   BlPitch(1)  - Blade 1 initial pitch (degrees)
          0   BlPitch(2)  - Blade 2 initial pitch (degrees)
          0   BlPitch(3)  - Blade 3 initial pitch (degrees) [unused for 2 blades]
          0   TeetDefl    - Initial or fixed teeter angle (degrees) [unused for 3 blades]
          0   Azimuth     - Initial azimuth angle for blade 1 (degrees)
       12.1   RotSpeed    - Initial or fixed rotor speed (rpm)
          0   NacYaw      - Initial or fixed nacelle-yaw angle (degrees)
          0   TTDspFA     - Initial fore-aft tower-top displacement (meters)
          0   TTDspSS     - Initial side-to-side tower-top displacement (meters)
          0   PtfmSurge   - Initial or fixed horizontal surge translational displacement of platform (meters)
          0   PtfmSway    - Initial or fixed horizontal sway translational displacement of platform (meters)
          0   PtfmHeave   - Initial or fixed vertical heave translational displacement of platform (meters)
          0   PtfmRoll    - Initial or fixed roll tilt rotational displacement of platform (degrees)
        0.1   PtfmPitch   - Initial or fixed pitch tilt rotational displacement of platform (degrees)
          0   PtfmYaw     - Initial or fixed yaw rotational displacement of platform (degrees)
```